AI-BASED SOLUTION TO THE OPTIMIZATION PROBLEM OF THE MICROFLUIDIC GEOMETRY DESIGN

2024, Novosibirsk, Russia

AI-BASED SOLUTION TO THE OPTIMIZATION PROBLEM OF THE MICROFLUIDIC GEOMETRY DESIGN

By Grigorev Georgii

Nikitin N.O.,
Hvatov A.,
Kalyuzhnaya A.V.

清华-伯克利深圳学院

Date: 7/October/2024

Report Outline

Roadmap Infographics

Literature Review
Problem statement.
Goals .

Proposal experimental verification
Chip for single cell inside-and-outside analysis .

Topology Optimization 1
MANUAL CREATION

Topology Optimization 2
Auto creation

Topology Optimization 3
Auto creation and improvement, 300.

Topology optimization 4
Auto creation and self improvement, 30,000

Final geometry experimental test
Results.

Review:

MICROFLUIDICS FOR SINGLE RBC STUDIES (492 REFS)

RBC SCA: Attention rises

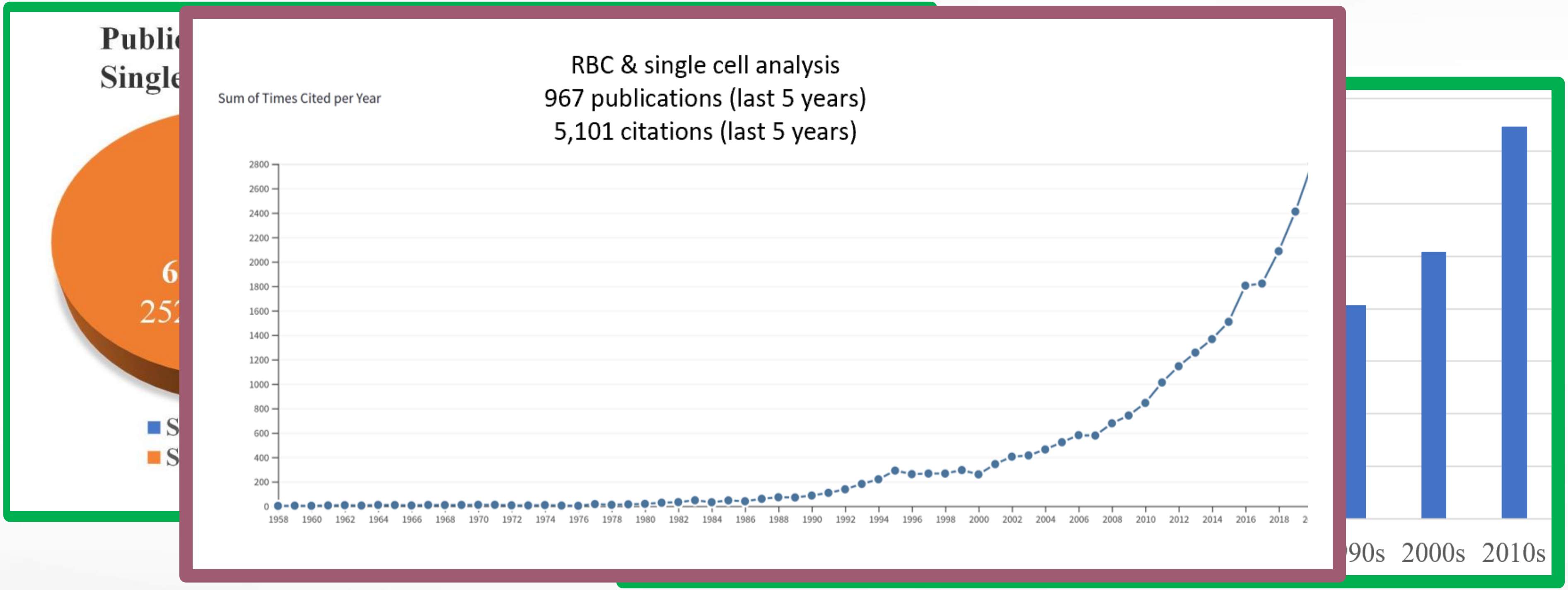

Grigorev et al. Biosensors **2022**, pending

Centers for Disease Control and Prevention
CDC 24/7: Saving Lives, Protecting People™

World Health Organization

Leading Causes of Death

eaths for leading causes of death

59,041

- Accidents (unintentional injuries): 173,040
- Chronic lower respiratory diseases: 156,979
- Stroke (cerebrovascular diseases): 150,005
- Alzheimer's disease: 121,499

otic syndrome, and nephrosis: 51,565

eumonia: 49,783

arm (suicide): 47,511

the United States, 2019, data table for figure 2

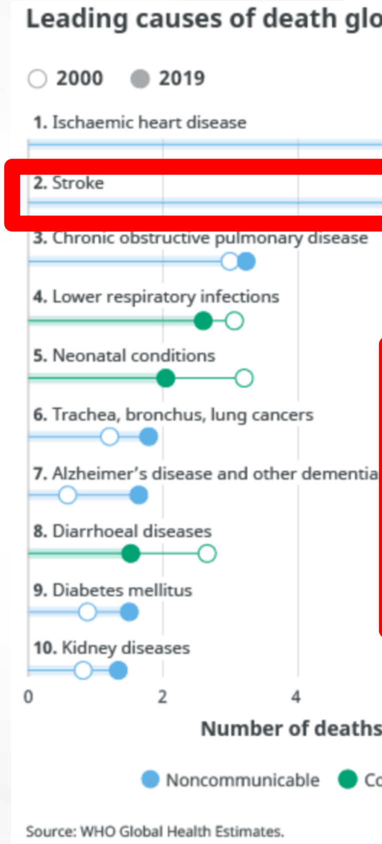

Video Credit: Shishova's Lab

Problem Statement

uFD Chip.

Biomicrofluidic chip,
suitable for visual, quantitative and qualitative study of single RBC inside and outside.

Trapping geometry.

Trap RBCs in channels while keeping them suspended to allow fluidic flows around the cell..

Topology Optimization.

Achieve trapping efficiency 75%.

SCA

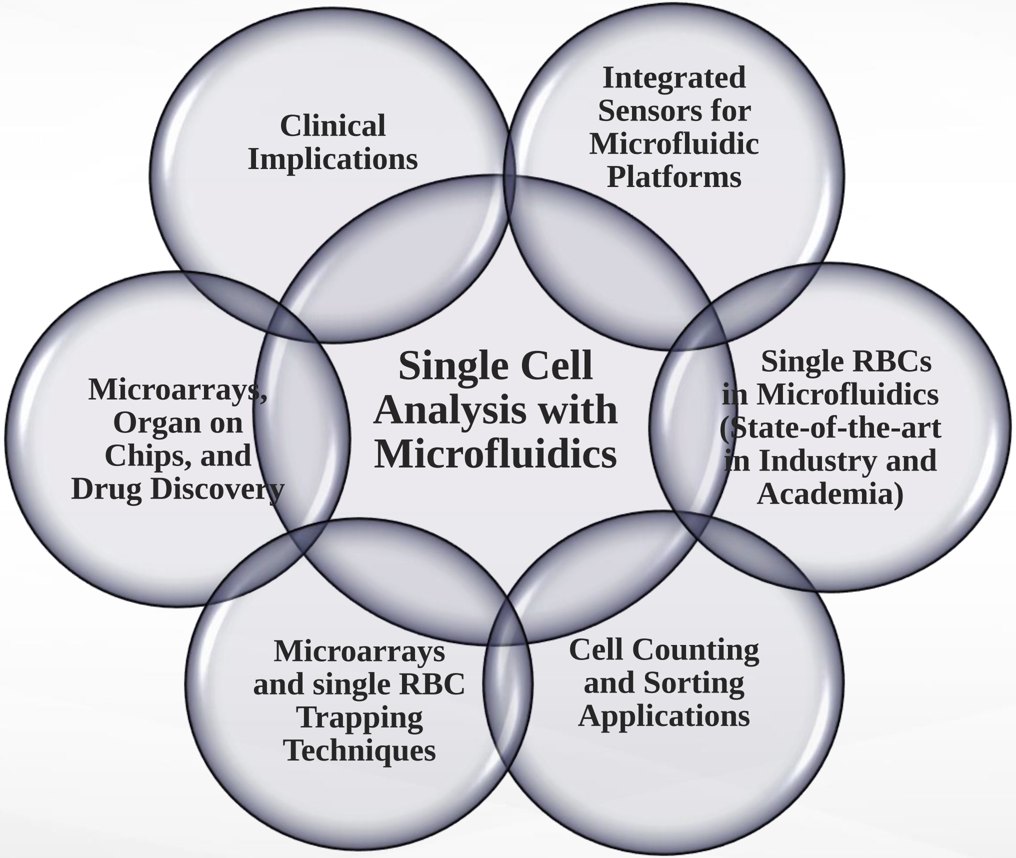
Clinical Implications
Integrated Sensors for Microfluidic Platforms
Microarrays, Organ on Chips, and Drug Discovery
Single Cell Analysis with Microfluidics
Single RBCs in Microfluidics (State-of-the-art in Industry and Academia)
Microarrays and single RBC Trapping Techniques
Cell Counting and Sorting Applications

Historical timeline of developments in materials and microfluidics

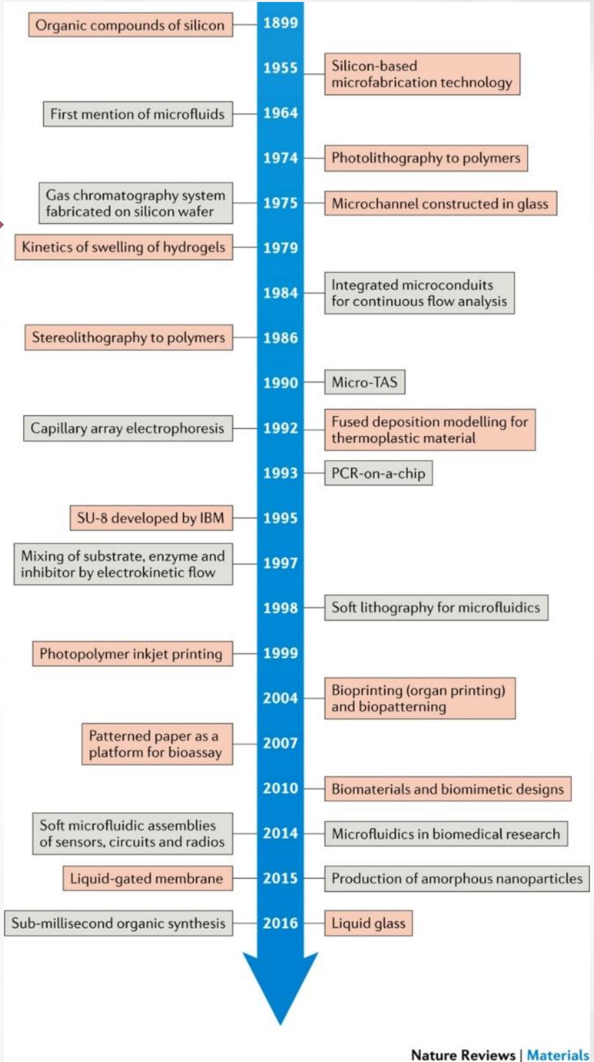

Hou, X. (2017) Interplay between materials and microfluidics
Nat. Rev. Mater. doi:10.1038/natrevmats.2017.16

Erythrocyte / RBC

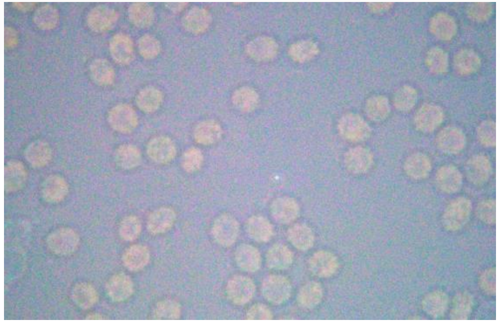

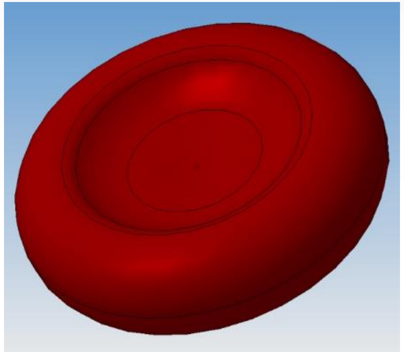

A mature erythrocyte has a biconcave discoid shape. An erythrocyte is composed of hemoglobin (32%), water (65%), and membrane components (3%) and does not contain any nucleus. P. Mazeron, S. Muller, and H. El. Azouzi, "Deformation of erythrocytes under shear: a small-angle light scattering study," Biorheology 34, 99-110 (1997).

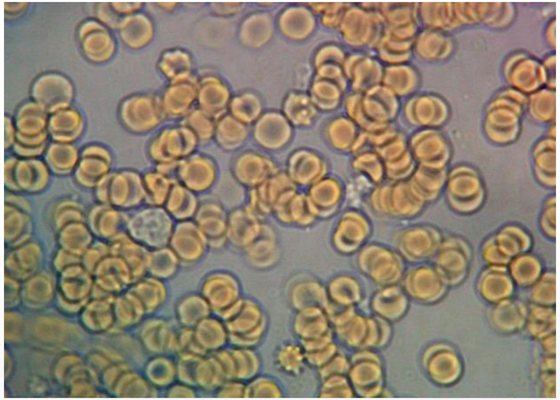

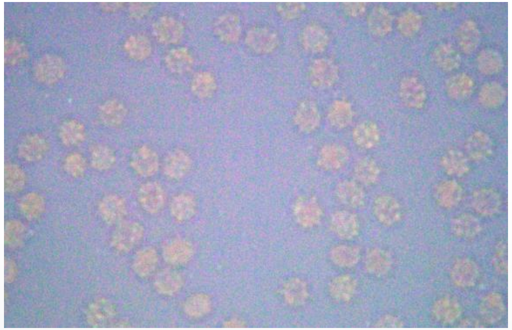

$$z^2 = \left(\frac{0.86d}{2}\right)^2\left[1-\left(\frac{2x}{d}\right)^2\right]\left[0.01384083 + 0.2842917\left(\frac{2x}{d}\right)^2 + 0.01306932\left(\frac{2x}{d}\right)^4\right].$$

*Grigorev et al. IEEE, RCAR **2019**, 531-536*

RBCs differ:

Depending on the value of the RBC's SC erythrocytes have different

shape:

- Spherocytes
- Elliptocytes/Ovalocytes
- Stomatocytes
- Schistocytes
- Keratocytes
- Helmet Cells
- Acanthocytes
- Echinocytes
- Target Cells (Codocytes)
- Tear Drop Cells (Dacryocytes)
- Sickle Cells (Drepanocytes)
- Degmacytes

size:

- Normocytes
- Anisocytosis
- Microcytes
- Macrocytes
- Megalocytes

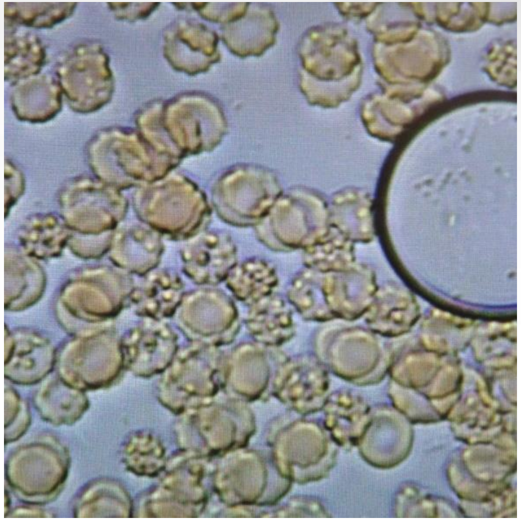

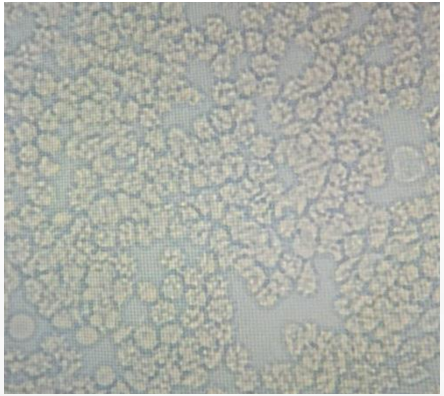

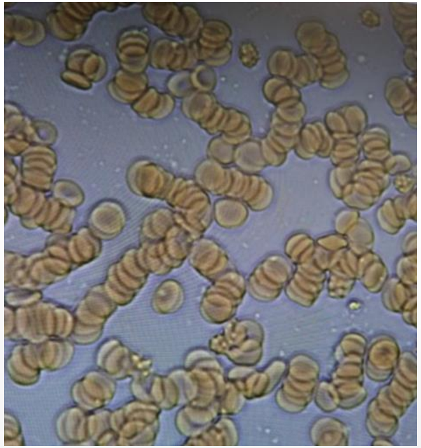

Grigorev et al. IEEE, RCAR **2019**, *531-536*

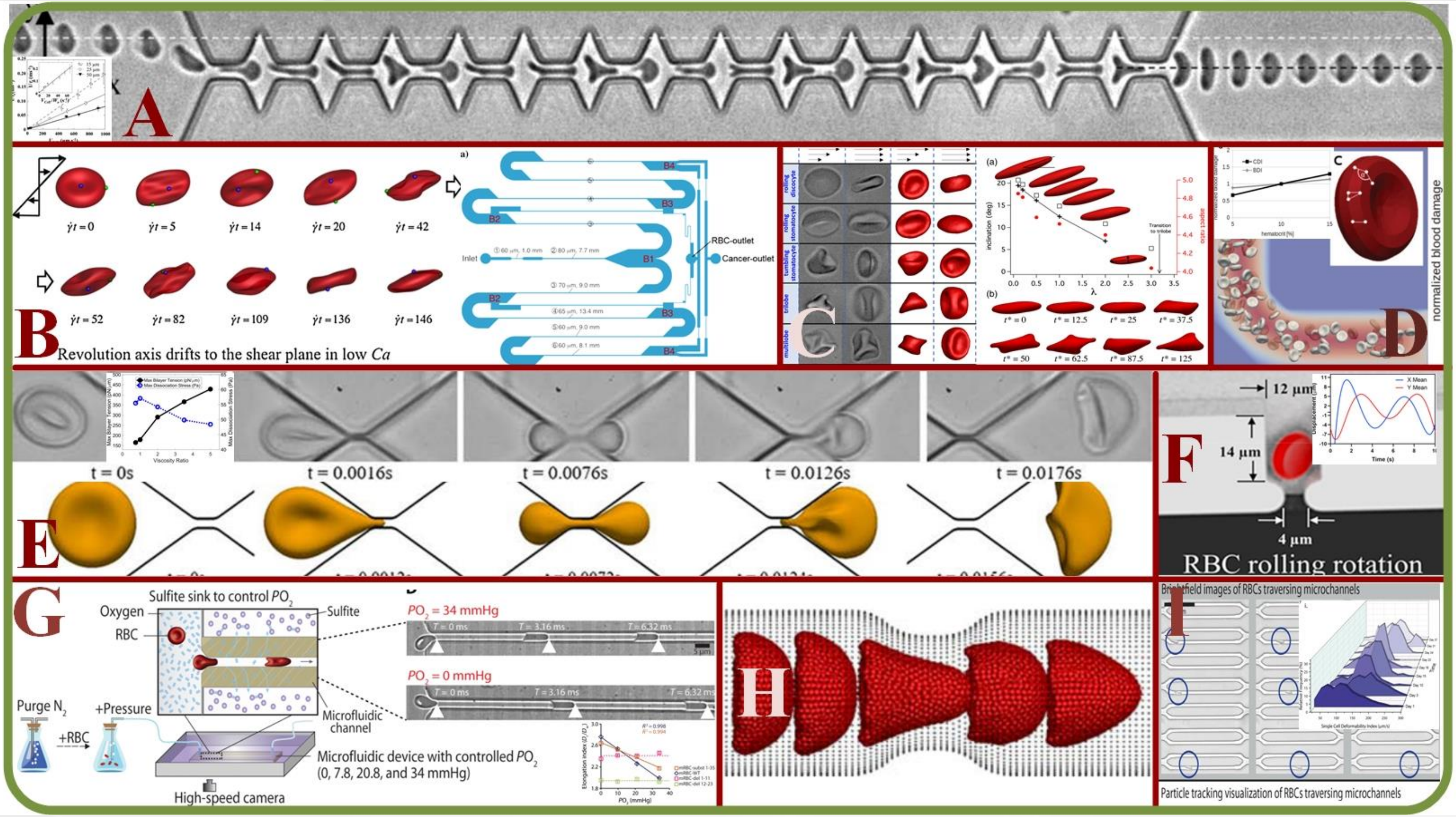

Reffs 72-89

Single RBC arrays

***Grigorev** et al. Review, Biosensors* **2022**, pending

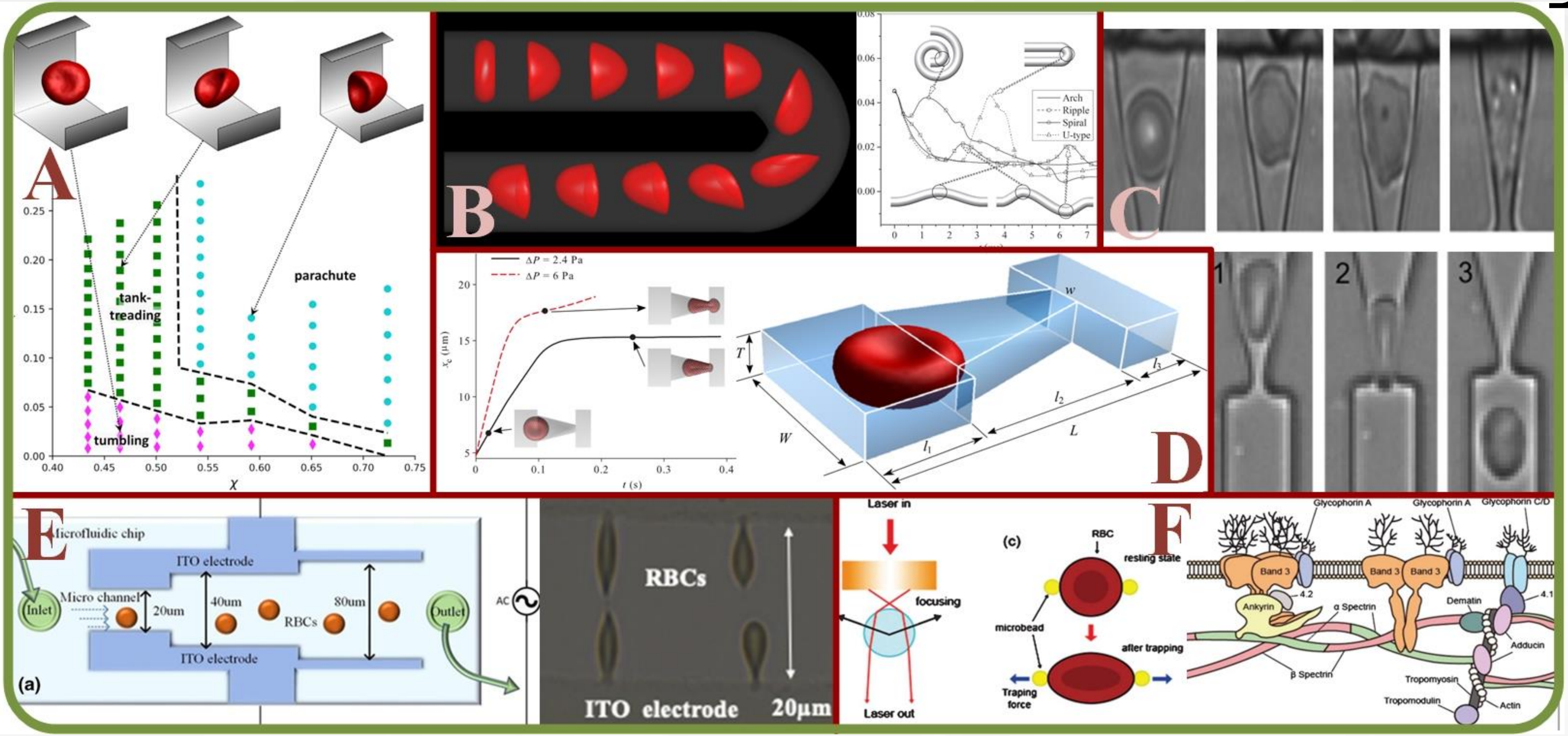

Reffs 129-142

Deformation of single Erythrocytes in Microchannels.

Grigorev et al. Review, Biosensors **2022**, pending

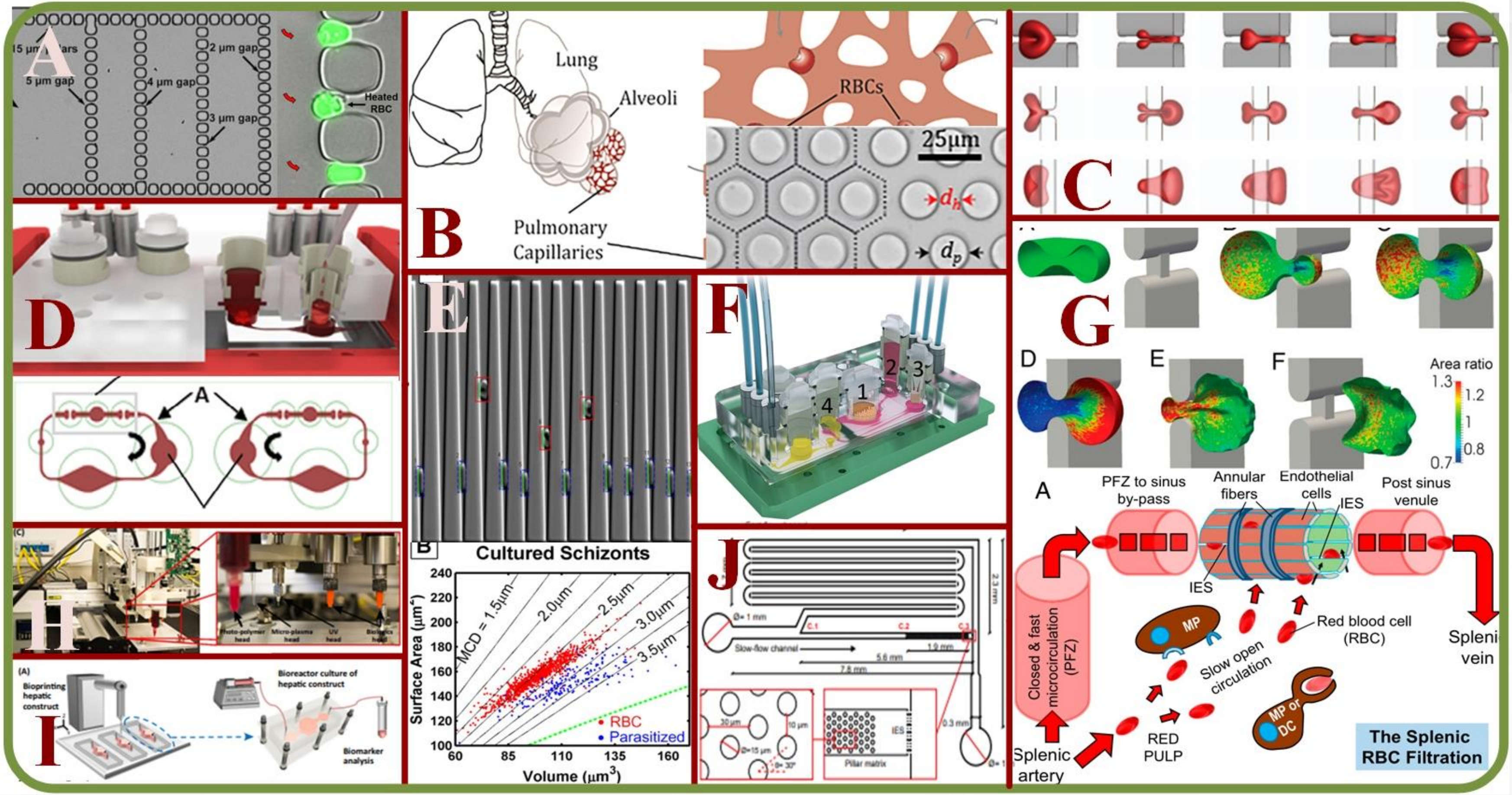

Reffs 377-392

Organ-On-Chips and Drug Discovery involving single RBCs

***Grigorev** et al. Review, Biosensors* **2022**, pending

Funding

₽ ¥ ₹ $

March 25, 2013

BOSTON — The Wyss Institute for Biologically Inspired Engineering at Harvard University announced today that it was awarded a **$9.25 million** contract from the Defense Advanced Research Projects Agency (DARPA) to further advance **a blood-cleansing technology** developed at the Institute with prior DARPA support, and help accelerate its translation to humans as a new type of sepsis therapy.

Funding

theranos

estimated value = 9,400,000,000$
USA Moon project = 20,400,000,000$

the board of the directors members (all-star board):

- William **Perry** (former Secretary of Defense)
- Henry **Kissinger** (former Secretary of State)
- Sam **Nunn** (former U.S. Senator)
- Bill **Frist** (former U.S. Senator and heart-transplant surgeon)
- Gary **Roughead** (Admiral, USN, retired)
- James **Mattis** (General, USMC)
- George P. **Schultz** (former Secretary of State)
- Richard **Kovacevich** (former Wells Fargo Chairman and CEO)
- Riley **Bechtel** (chairman of the board and former CEO at Bechtel Group)
- William **Foege** (former director U.S. Centers for Disease Control and Prevention) and others

http://www.businessinsider.com/theranos-founder-elizabeth-holmes-is-a-billionaire-2014-9

Table 1 : Common Microfluidic Separation Methods

Method	Advantages	Disadvantages
Physical filtration	Increased cell separation and sorting efficiency, easily integrated with PDMS structures	Clogging and fouling of blood cells requires precise control of filter geometries
Hydrodynamic and hemodynamic processes	Inertial focusing for enhanced cell separation and sorting narrowed sheathed flows	Produce stress on cell samples, may alter molecular mechanisms, inhomogeneity
Surface Affinity and Topography	Specificity, cell purity	May alter cell physiology after sorting and isolation processes
Magnetophoresis	Directly differentiate blood cells without additives, efficiency up to ~ 90 %	Weak magnetic flux gradients on cells
Electrical Methods and Acoustophoresis	Sensitive, rapid, convenient, and robust. Easily integrated	Electrolysis, temperature elevations, phenotypic changes

***Grigorev** et al. Biosensors* **2022**, pending

Innovation

Research Objectives

Objective #1, uFD Chip

Biomicrofluidic chip, suitable for visual, quantitative and qualitative study of single RBC inside and outside

Objective #2, Trapping geometry

Trap RBCs in channels while keeping them suspended to allow fluidic flows around the trapped cell.

Objective #3, Topology Optimization

Achieve trapping efficiency 75%

CHIP DESIGN; EXPERIMENTAL TEST OF CAPABILITIES FOR SINGLE CELL ANALYSIS

Experimental results and discussion

Local Optical Tomography

- Design and fabricate microfluidic chip suitable for LOT
- Run the RBC solution through the chip and trap at least one cell
- Mathematically restore the 3D surface of the trapped RBC (RBCs surface vary per RBC type)

Raman spectrometry

- Design and fabricate microfluidic chip suitable for Raman spectrometry
- Run the RBC solution through the chip and trap at least one cell
- Obtain spectra of the chip + trapped RBC
- Clearly detect hemoglobin on the spectra

Concept

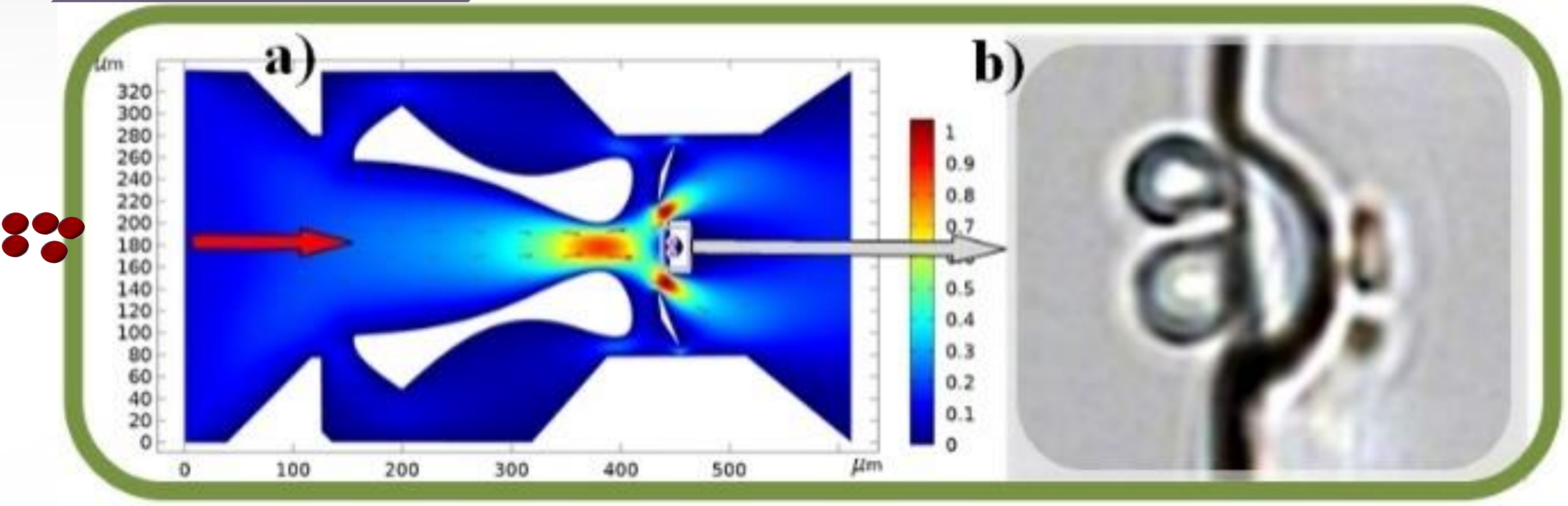

Simulation and trapping.

a) COMSOL simulation of the velocity gradient distribution in the trapping chamber (inflow velocity = 0.1 m/s, no slip boundary condition), red arrow indicates the flow direction;

b) 2 RBCs trapped in the mid-section cavity of the chamber and ready for tests.

Grigorev et al. Mendeleev Comms, **2022**, *3 (accepted)*

Fabrication

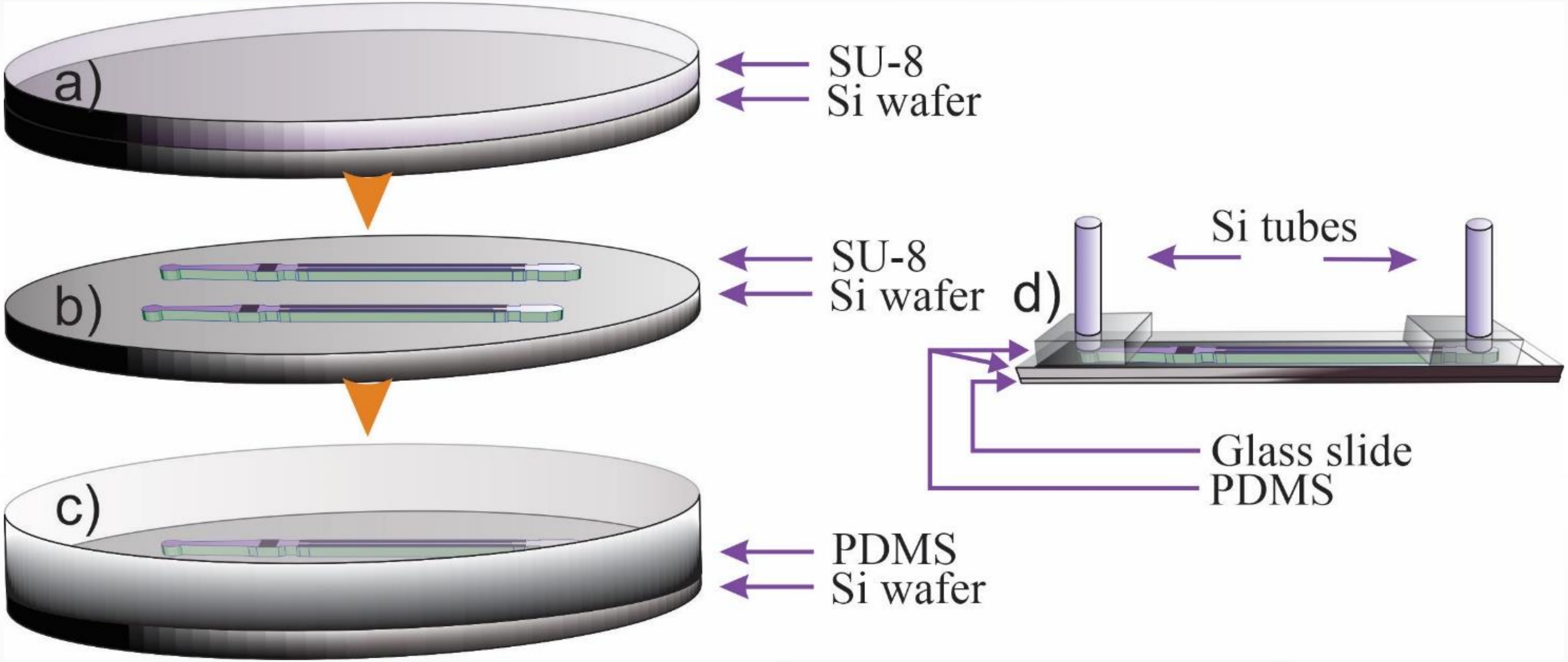

Figure: chip fabrication

a) photoresist spincoating; b) photolitoghraphy;
c) PDMS mold; d) chip packaging

Grigorev *et al. Micromachines* **2022**, *13*(3), 367

Local optical tomography by differential projections

pe have a

an **internal**

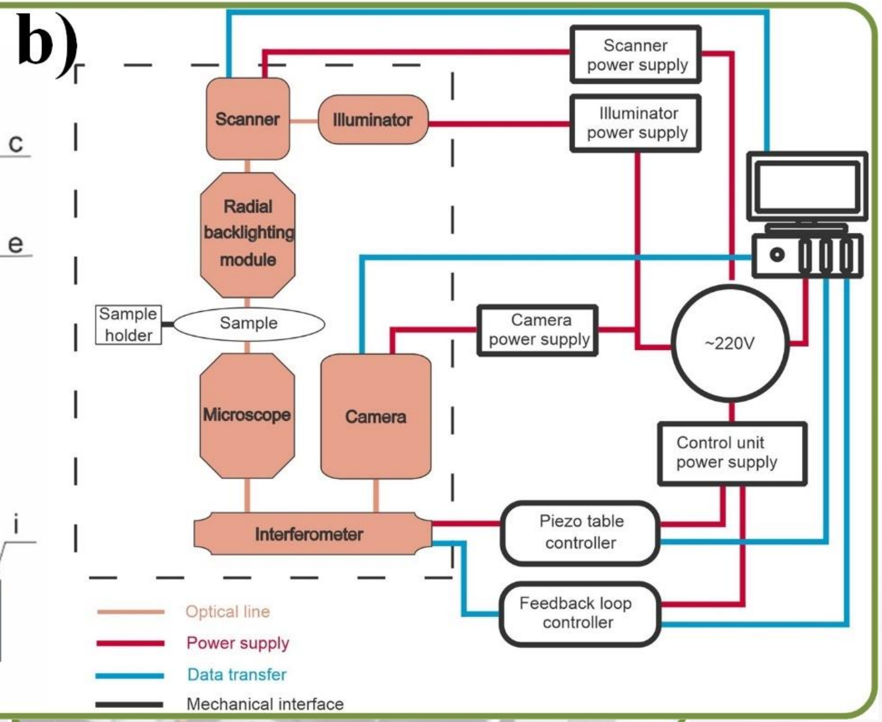

Whole image from the DIC-projections (1) is proportional to the Hilbert transform of the original function of the object. Applying inverse Hilbert transform (2) to DIC-projections image the tomogram of an object is reconstructed [10.1134/S0030400X18120226].

$$b(x,z) = -2\pi H_x[f(x,z)]$$

$$f(x,z) = \frac{1}{2\pi} H_x[b(x,z)]$$

$$b(x,z) = \int_{-\frac{\pi}{2}}^{+\frac{\pi}{2}} g(x\cos\varphi + z\sin\varphi; \varphi)\, d\varphi$$

is total image from the DIC projections, $f(x,z)$ is 2D image,

φ is the angle between the perpendicular and the x axis on the interval $[-\frac{\pi}{2}, +\frac{\pi}{2}]$

H_x – Hilbert transform operator by x-axis and

g is a partial derivative of the 1st order (r-coordinate) of central section

LOT

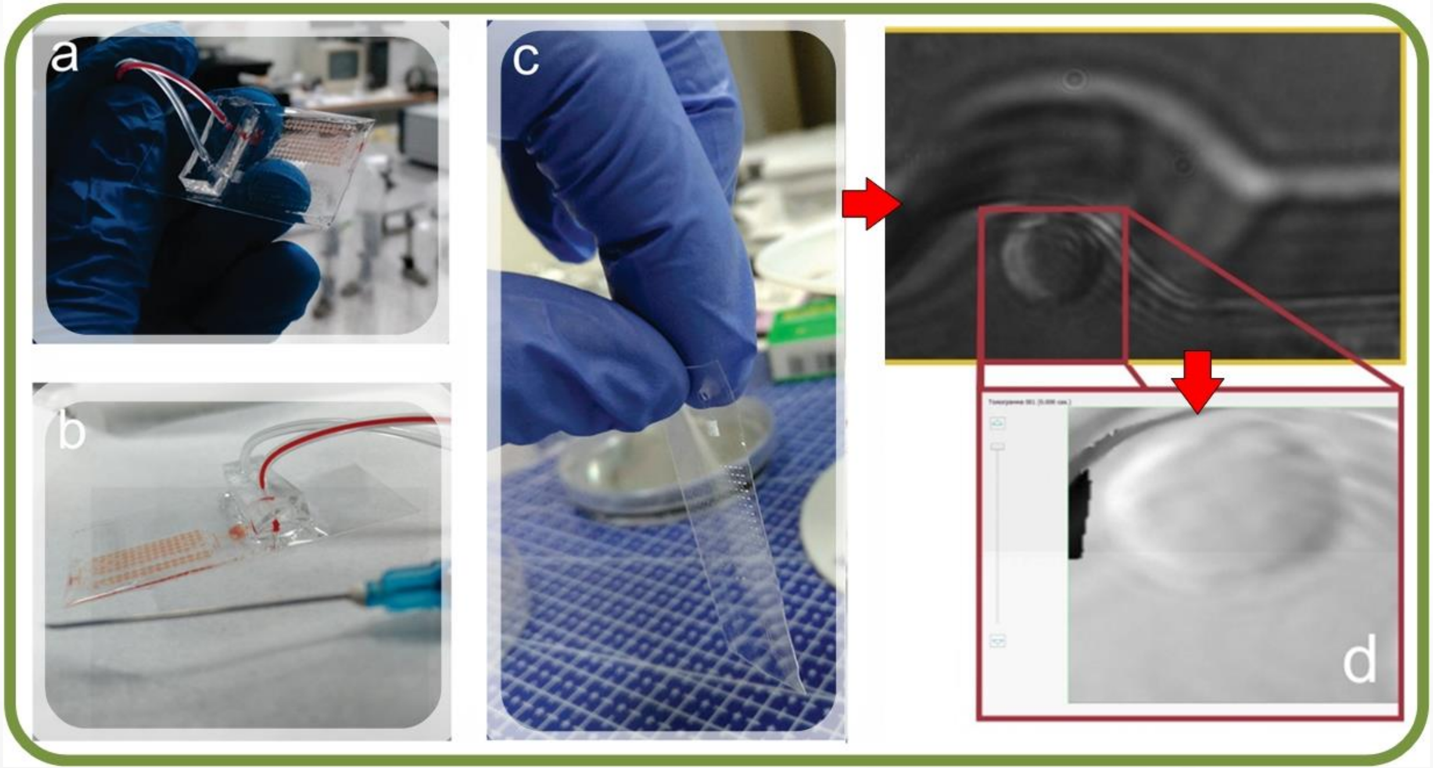

Typical fabricated microfluidic device

a) chip with one line used for blood solution being injected, due to the limitations of the Local Optical Tomograph the overall thickness is limited by 300 μm and output flow should be open, having no tubes or secondary PDMS slabs on top of it; b) device thickness comparison to a 0.6 mm thick medical syringe injector needle; c) – an example of a PDMS first layer film used for LOT

***Grigorev** et al. Mendeleev Comms,* **2022**, *3 (accepted)*

Results of Raman spectrometry (combinatorial scattering)

Raman shift, cm^{-1}	Chemical bonds	The sensitivity of band
1640	C_aC_m, C_aC_mH, C_aC_b	Redox and spin state of Fe, presence of ligand
1588-1580	C_aC_m, C_aC_mH	Spin state of heme Fe, diameter of porphirin ring
1552	C_aC_m, C_aC_mH	Spin state of heme Fe, diameter of porphirin ring

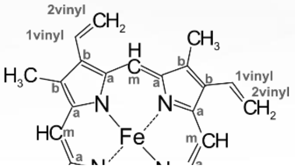

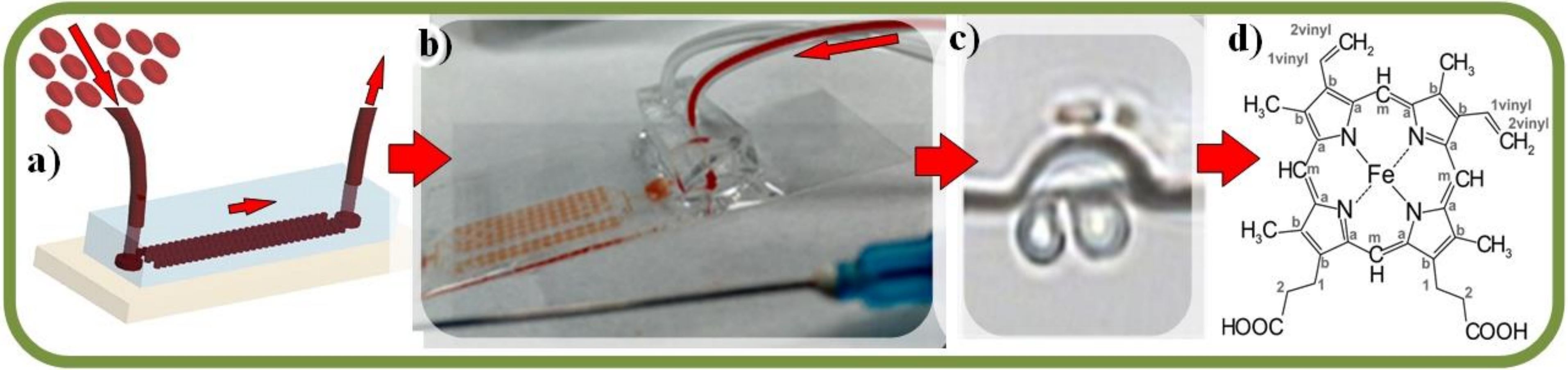

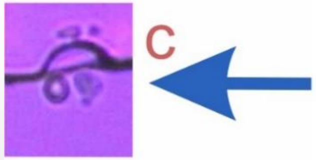

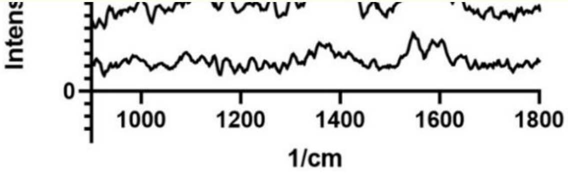

Grigorev et al. Mendeleev Comms, **2022**, *3*

TOP. OPT. 1: OF MINIMIZATION. MANUAL CREATION/TESTING OF NEW GEOMETRIES

Hydrodynamic RBC SiCMA

- **Design**: Glass (1.01; 0.17 mm) + PDMS (4.8; 0. 13 mm) round chamber (1 mm), V-shaped trap, holding/capturing concavity *d* = 25/35 micron (15 columns, 8 rows, 2 channels per chip == 240 chambers).

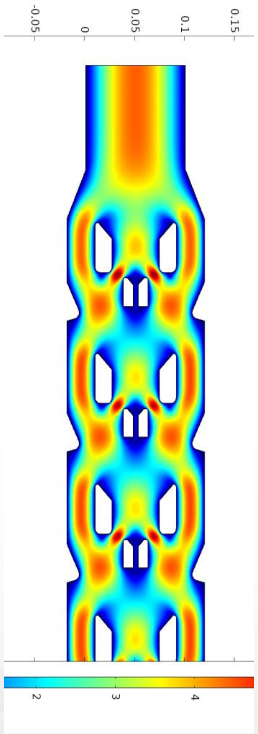

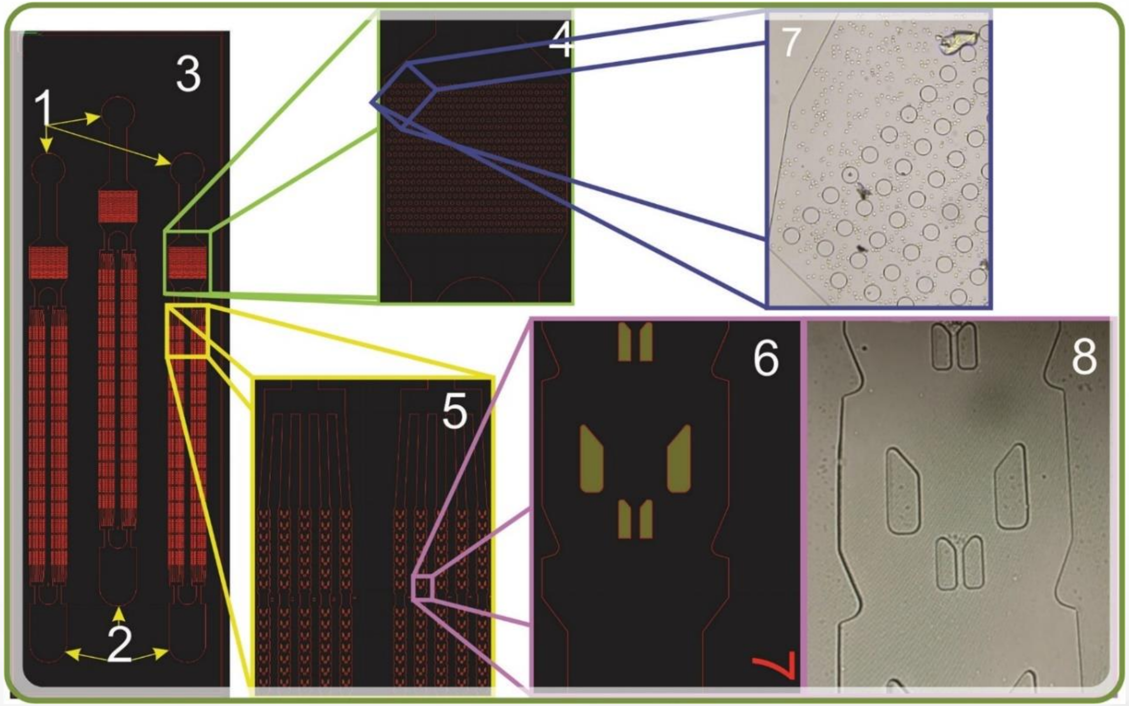

Typical geometry of the devices used in the experiments for establishing the optimal width of the trapping channels.

Fabrication

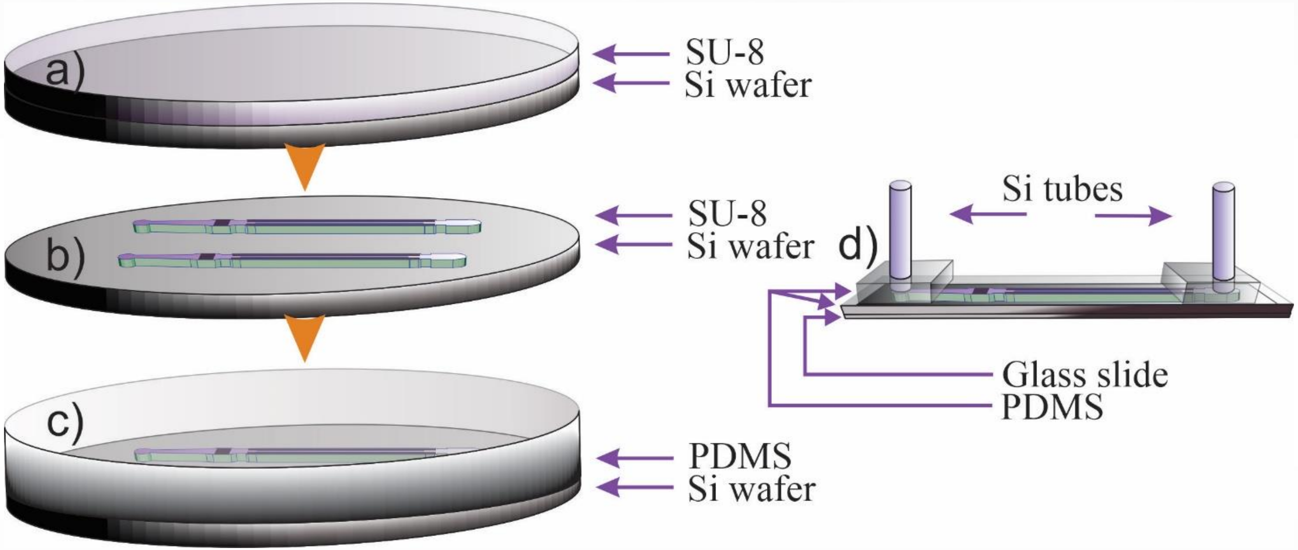

Figure: chip fabrication

a) photoresist spincoating; b) photolitoghraphy;
c) PDMS mold; d) chip packaging

***Grigorev** et al. Micromachines* **2022**, *13*(3), 367

Experimental microscopic images of establishing the optimal trapping width for trapping a target cell.

f, g, h – bovine erythrocytes, a, b, c, d, e – human RBCs. To find the optimal parameters of a trap different geometries were tested within one chip: width ranging from 1 µm to 8 µm. a) 8 µm; b) 7 µm; c) 6 µm; d) 5 µm; e) 4 µm; f) 3 µm; g) 2 µm; h) 1 µm; the diameter of the human RBC = 7-8 µm [462], the size of the bovine RBC = 5-6 µm[474]

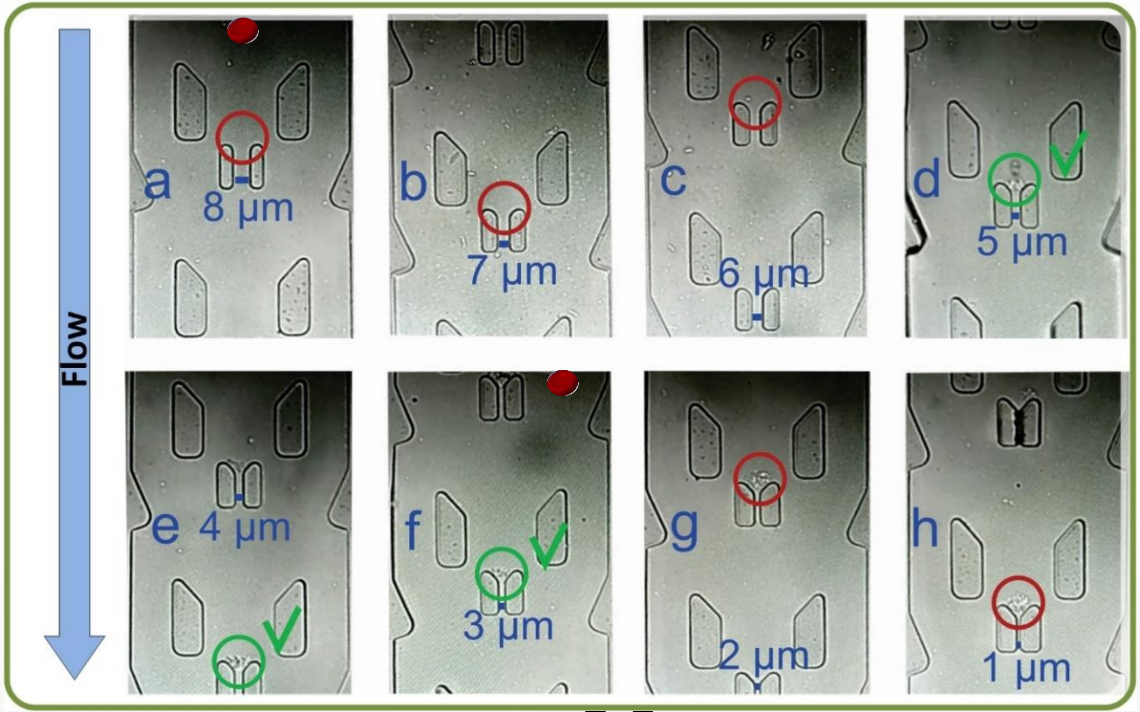

Flow solution rheological parameters (blood density…)

f_large	intop1(u)	m²/s	Flow rate through the large outlet
f_1	intop2(u)	m²/s	Flow rate through the small outlet
f_2			Flow rate ratio
alpha			Friction force
target_f_large			Target flow rate 1
target_f_small			Target flow rate 2
volume_f			olume fraction of the material
obj	(f_1 - 1)^2		Objective function
f_3			
curl			
f_4			
f_5			
Re			Reynolds number
mu0			Dynamic viscosity
rho0			Density
D			Inlet width
Uin			Average inlet velocity
meshsz	0.0005[mm]	5E-7 m	Mesh size

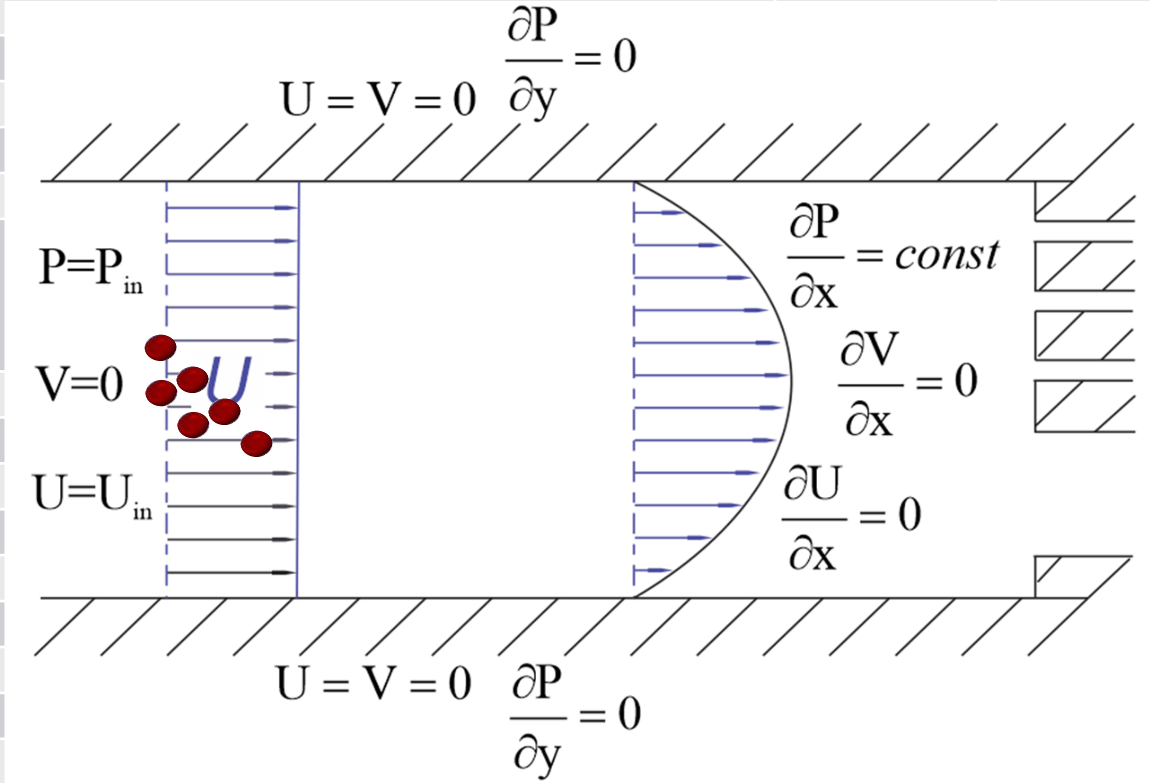

Objective function	Flow rates, units = 10^{-6} м²/s			
	Broad channel F_0	1-st channel	2-nd channel	3-rd channel
0 (optimization off)	95.8	1.37	1.38	1.39
$(F_1 / T_1 - 1)^2 + (F_2 / T_2 - 1)^2 + (F_3 / T_3 - 1)^2 + 4(F_0 / T_0 - 1)^2$ $T_1 = T_2 = T_3 = 40.0$ $T_0 = 100.0$	58.9	13.7	13.7	13.7

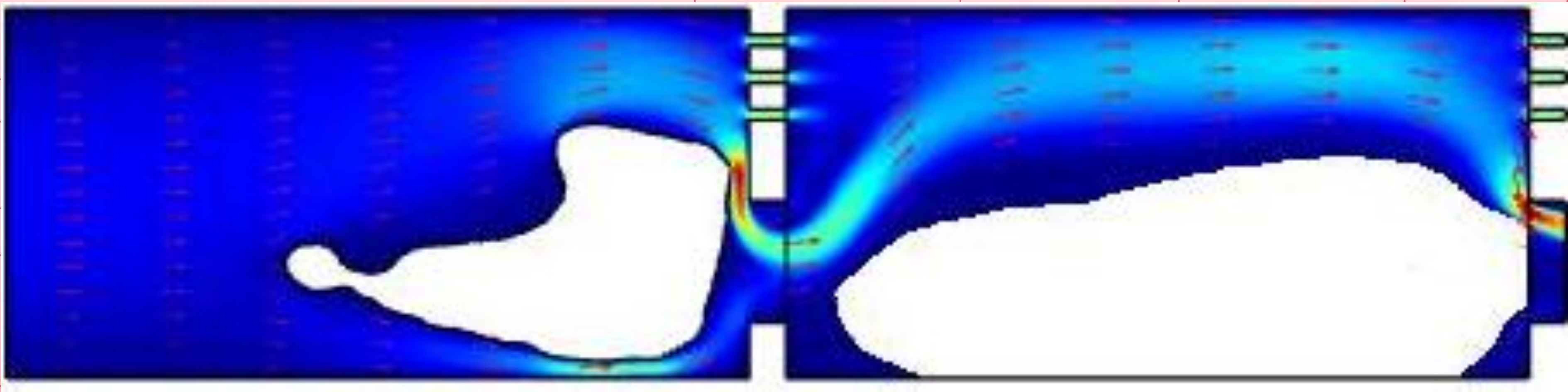

$$= \left(\frac{\int_{narrow\_channel\_1} u\ dl}{target_{f_{narrow}}} - 1\right)^2 + \left(\frac{\int_{narrow\_channel\_2} u\ dl}{target_{f_{narrow}}} - 1\right)^2 + \left(\frac{\int_{narrow\_channel\_3} u\ dl}{target\_f_{narrow}} - 1\right)^2 + 4 * \left(\frac{f_{broad}\, dl}{target\_f_{broad}} - 1\right)^2 \quad (3.1)$$

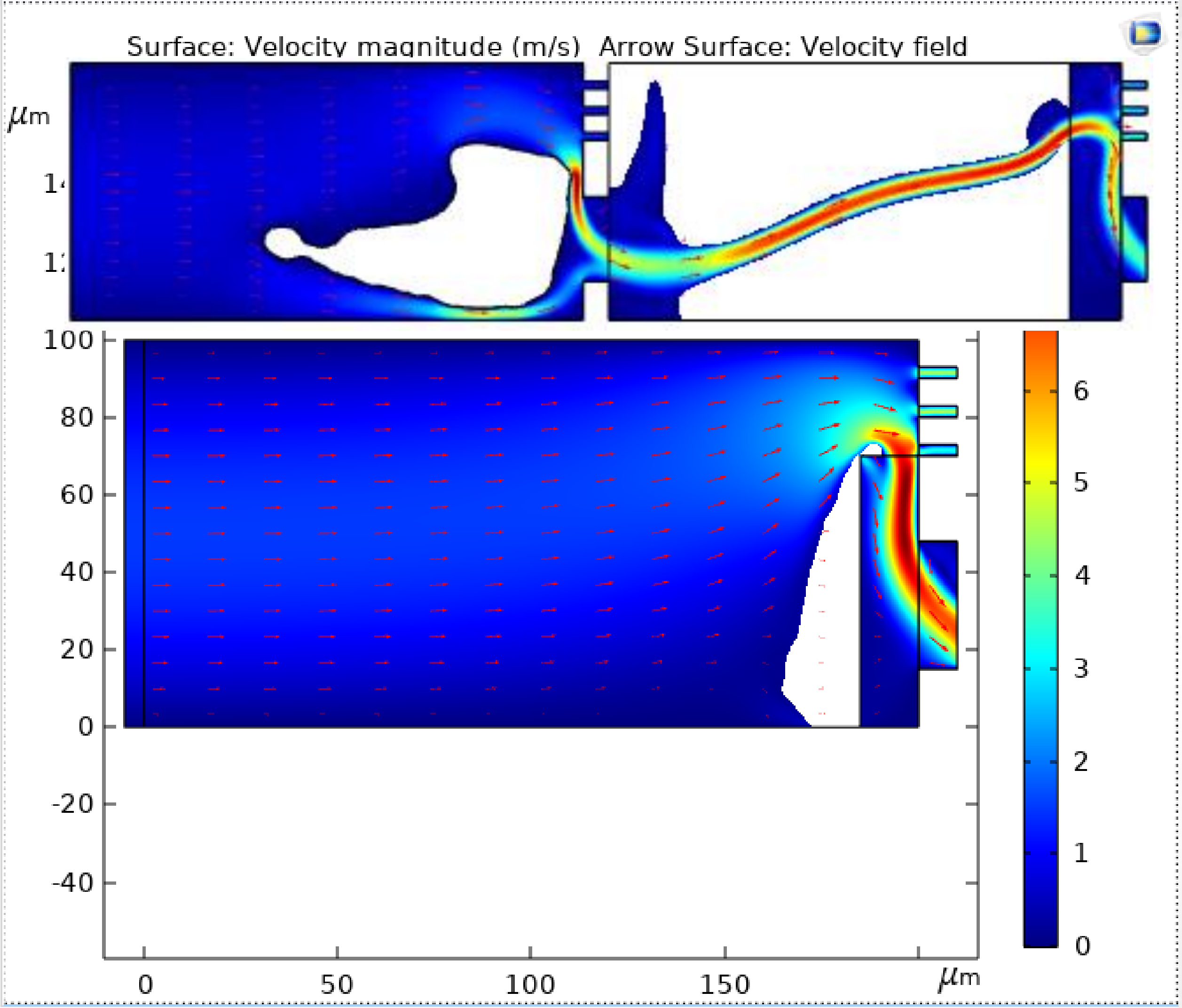
Surface: Velocity magnitude (m/s) Arrow Surface: Velocity field
μm
100
80
60
40
20
0
-20
-40
0
50
100
150
μm
6
5
4
3
2
1
0

Constraints

$$CRV = \iint abs\left[\frac{u^2 * \frac{\partial v}{\partial x} - v^2 \frac{\partial u}{\partial y} + uv * \left(\frac{\partial v}{\partial y} - \frac{\partial u}{\partial x}\right)}{(u^2 + v^2)^{3/2}}\right] dxdy$$

$$OF = \left(\frac{\int_{narrow\_channel\_1} u\ dl}{target_{f\ narrow}} - 1\right)^2 + \left(\frac{\int_{narrow\_channel\_2} u\ dl}{target_{f\ narrow}} - 1\right)^2 + \left(\frac{\int_{narrow\_channel\_3} u\ dl}{target\_f_{narrow}} - 1\right)^2 + \left(\frac{\int_{narrow\_channel\_4} u\ dl}{target\_f_{narrow}} - 1\right)^2 + \left(\frac{\int_{narrow\_channel\_5} u\ dl}{target\_f_{narrow}} - 1\right)^2 + k * \left(\frac{f_{broad}\, dl}{target\_f_{broad}} - 1\right)^2$$

$$
\begin{aligned}
OF &= \left(\frac{\int_{narrow\_channel\_1} u \; dl}{target_{f\;narrow}} - 1\right)^2 + \left(\frac{\int_{narrow\_channel\_2} u \; dl}{target_{f\;narrow}} - 1\right)^2 \\
&+ \left(\frac{\int_{narrow\_channel\_3} u \; dl}{target\_f_{narrow}} - 1\right)^2 + \left(\frac{\int_{narrow\_channel\_4} u \; dl}{target\_f_{narrow}} - 1\right)^2 \\
&+ \left(\frac{\int_{narrow\_channel\_5} u \; dl}{target\_f_{narrow}} - 1\right)^2 + k * \left(\frac{f_{broad}\, dl}{target\_f_{broad}} - 1\right)^2 \\
&+ \left(\frac{\max_{\Omega}\left(\frac{\partial u}{\partial y}\right) + \max_{\Omega}\left(\frac{\partial v}{\partial x}\right)}{target\_CRL} - 1\right)^2 \\
&+ \left(\frac{\iint_{\Omega} abs\left[\frac{u^2 * \frac{\partial v}{\partial x} - v^2 \frac{\partial u}{\partial y} + uv * \left(\frac{\partial v}{\partial y} - \frac{\partial u}{\partial x}\right)}{(u^2 + v^2)^{3/2}}\right] dxdy}{target\_CRV} - 1\right)^2
\end{aligned}
$$

Constraints

CRL = maxop1(uy) + maxop1(vx)

$$\max_{\Omega}\left(\frac{\partial u}{\partial y}\right) + \max_{\Omega}\left(\frac{\partial v}{\partial x}\right)$$

CRV = intop1(abs(u^2 * vx - v^2 * uy + u*v*(vy - ux))/(u^2 + v^2)^1.5)

$$\iint_{\Omega} abs\left[\frac{u^2 * \frac{\partial v}{\partial x} - v^2\frac{\partial u}{\partial y} + uv * \left(\frac{\partial v}{\partial y} - \frac{\partial u}{\partial x}\right)}{(u^2+v^2)^{3/2}}\right] dxdy$$

Grigorev *et al. Micromachines* **2022**, *13*(3), 367

OF topology optimization

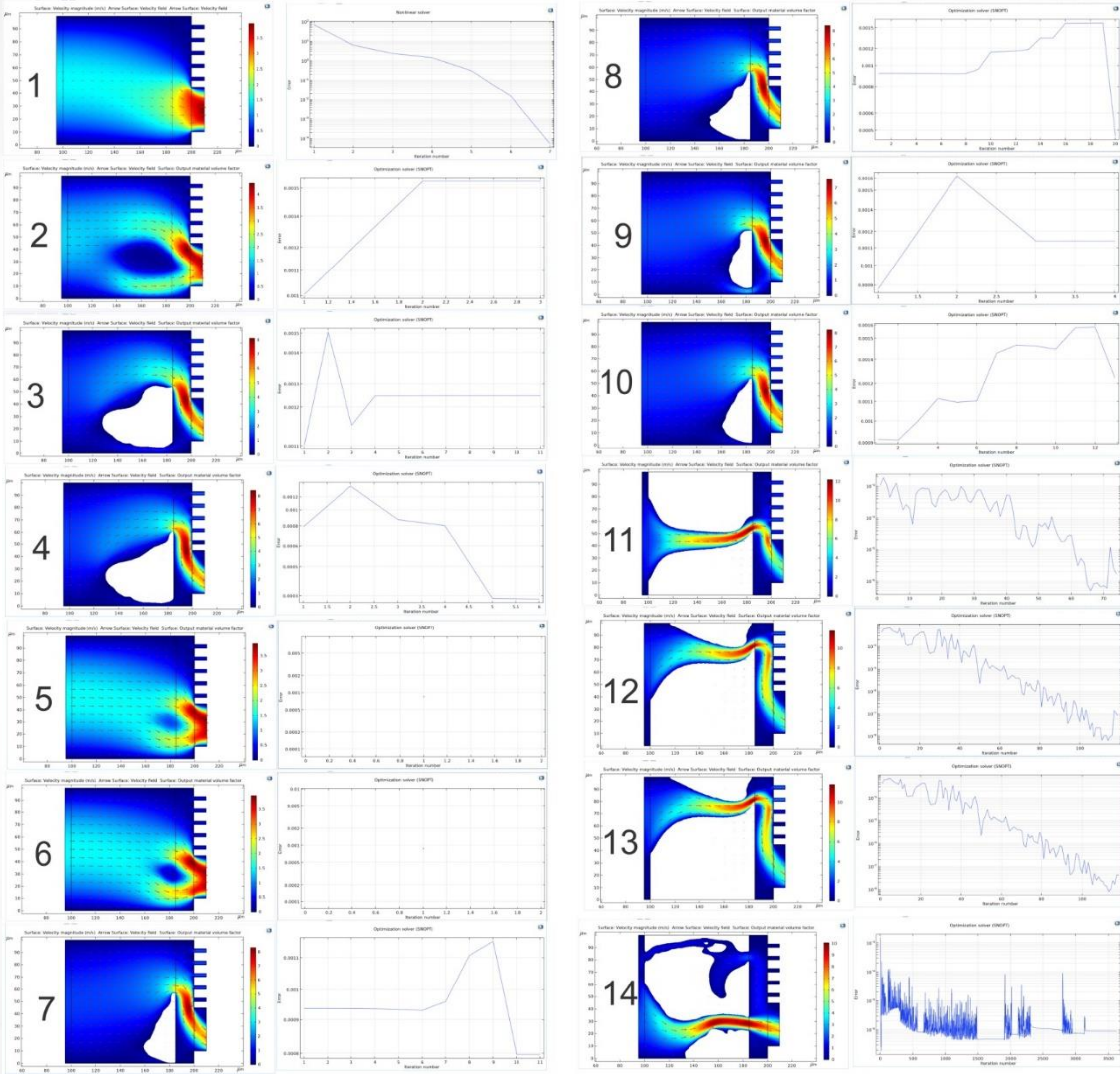

Pareto front parametrical plot

coefficients for the parts of the OF OF=K_1*()+K_2*()...			Target values				Probed value after the simulation					simulation NN
F_Broad	curl	curvature	target_f_small	target_curl	target_curvature	target_f_broad	F_1	F_5	curl	curvature	F_broad	
4.0	1.0	8.0	4E-5[m^2/s]	2.00E+07	2E8[1/m]	1E-4[m^2/s]	5.96E-07	5.46E-07	3.23E+06	1.00E+08	9.71E-05	1
3.0	2.0	5.0	4E-5[m^2/s]	2.00E+07	2E8[1/m]	1E-4[m^2/s]	1.06E-06	8.20E-07	8.51E+06	2.06E+08	9.50E-05	2
2.0	4.0	2.0	4E-5[m^2/s]	2.00E+07	2E8[1/m]	1E-4[m^2/s]	2.98E-06	1.36E-06	1.11E+07	1.50E+08	8.72E-05	3
8.0	8.0	0.5	4E-5[m^2/s]	2.00E+07	2E8[1/m]	1E-4[m^2/s]	3.65E-06	1.09E-06	1.12E+07	2.25E+08	8.53E-05	4
2.0	2.0	15.0	4E-5[m^2/s]	2.00E+07	2E8[1/m]	1E-4[m^2/s]	8.03E-07	7.25E-07	7.90E+06	1.50E+08	9.60E-05	5
0.5	20.0	40.0	4E-5[m^2/s]	2.00E+07	2E8[1/m]	1E-4[m^2/s]	8.72E-07	7.79E-07	8.54E+06	9.43E+07	9.57E-05	6
0.5	2.0	4.0	4E-5[m^2/s]	2.00E+07	2E8[1/m]	1E-4[m^2/s]	3.44E-06	1.39E-06	1.18E+07	1.82E+08	8.54E-05	7
0.2	4.0	6.0	4E-5[m^2/s]	2.00E+07	2E8[1/m]	1E-4[m^2/s]	3.45E-06	1.52E-06	1.21E+07	1.95E+08	8.51E-05	8
0.1	10.0	8.0	4E-5[m^2/s]	2.00E+07	2E8[1/m]	1E-4[m^2/s]	2.68E-06	1.47E-06	1.10E+07	9.90E+07	8.80E-05	9
0.6	0.7	0.8	4E-5[m^2/s]	2.00E+07	2E8[1/m]	1E-4[m^2/s]	3.34E-06	1.53E-06	1.20E+07	1.72E+08	8.55E-05	10
1.0	0.0	0.0	4E-5[m^2/s]	2.00E+07	2E8[1/m]	1E-4[m^2/s]	4.22E-06	3.94E-06	1.84E+07	2.70E+08	7.85E-05	11
1.0	0.0	0.0	4E-5[m^2/s]	2.00E+07	2E8[1/m]	1E-4[m^2/s]	5.58E-06	5.79E-07	1.43E+07	3.54E+07	8.42E-05	12
1.0	0.0	0.0	4E-5[m^2/s]	2.00E+07	2E8[1/m]	1E-4[m^2/s]	5.58E-06	5.79E-07	1.43E+07	3.54E+07	8.42E-05	13
1.0	0.0	0.0	4E-6[m^2/s]	2.00E+07	2E8[1/m]	1E-5[m^2/s]	4.22E-06	3.92E-06	1.84E+07	1.42E+08	7.85E-05	14
1.0	0.0	0.0	4E-7[m^2/s]	2.00E+07	2E8[1/m]	1E-3[m^2/s]	4.00E-07	3.58E-08	3.66E+06	1.10E+08	9.88E-05	15
1.0	1.0	1.0	4E-6[m^2/s]	2.00E+07	2E8[1/m]	1E-4[m^2/s]	3.50E-06	1.04E-06	1.09E+07	2.00E+08	8.59E-05	16
1.0	20.0	20.0	4E-4[m^2/s]	2.00E+07	2E8[1/m]	1E-6[m^2/s]	4.21E-06	3.97E-06	1.85E+07	2.14E+08	7.85E-05	17

TOP. OPT. 2: AUTO CREATION/TESTING OF NEW GEOMETRIES (10, 000 DATASETS).

Constraints & variables

Constraints:

- flow curvature, flow width, flow rates.
- flow curvature (no flow direction rapid changes);
- flow width within the channel/chamber (the limit is - not narrower than ¼ or 1/3 of “broad channel” width;
- flow rates (each “narrow outlet” has 1/3 of a “broad outlet” flow rate).

Parameters that may vary within a range:

- width of the whole chamber (50 ... 250 microns);
- length of the whole chamber (10 … 200 microns) excluding outlets length;
- number of narrow outlet channels (3 ... 15);
- width of the broad outlet channel (50 ... 100 microns);
- length of the narrow and broad outlets (2 … 50 microns).

Topology Optimization 2

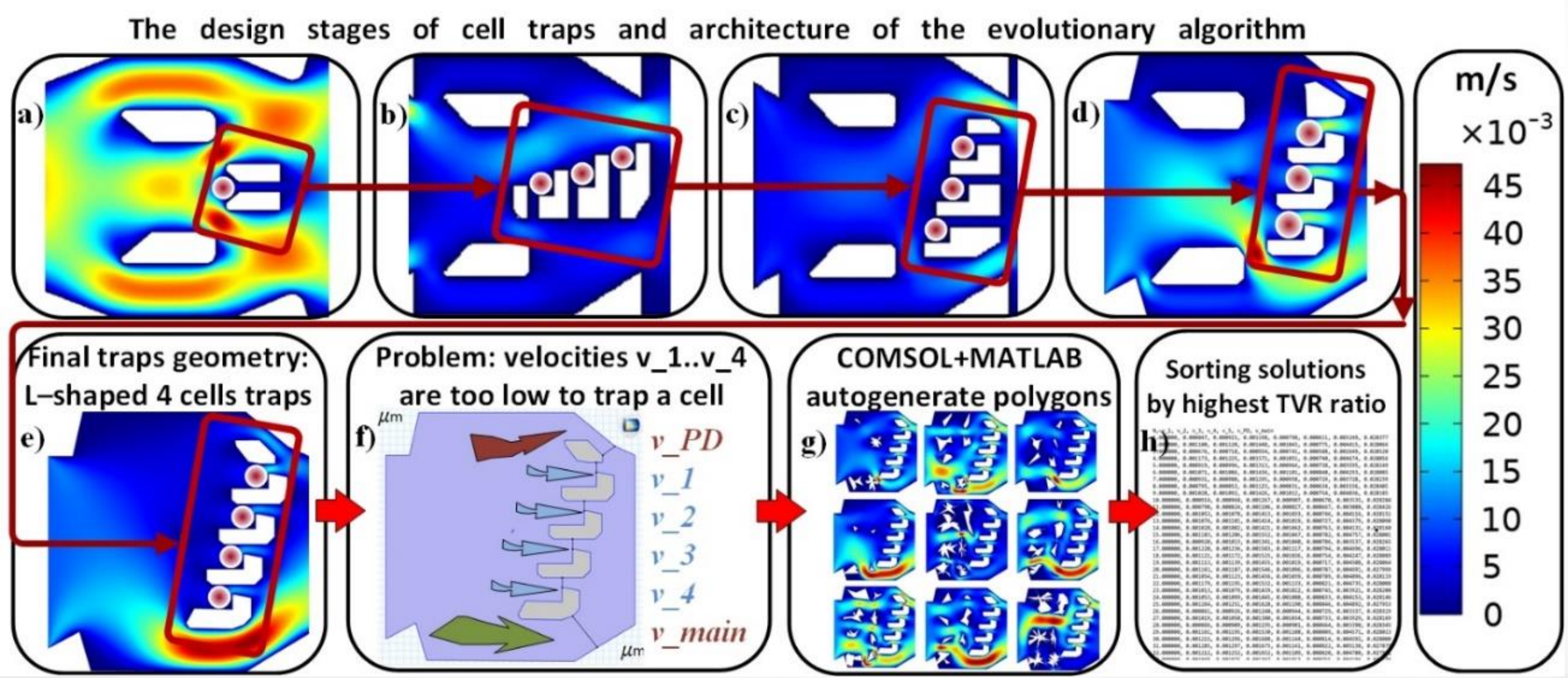

Grigorev *et al. Micromachines* **2022**, *13*(3), 367

N	v_1	v_2	v_3	v_4	v_5	v_PD	v_main
1.000000	0.000847	0.000921	0.001198	0.000798	0.000611	0.003249	0.028377
2.000000	0.001100	0.001120	0.001448	0.001043	0.000775	0.004415	0.028066
3.000000	0.000676	0.000718	0.000954	0.000741	0.000588	0.002649	0.028520
4.000000	0.001173	0.001225	0.001571	0.001051	0.000740	0.004674	0.028056
5.000000	0.000919	0.000996	0.001313	0.000964	0.000738	0.003595	0.028249
6.000000	0.001071	0.001086	0.001436	0.001101	0.000840	0.004293	0.028085
7.000000	0.000931	0.000980	0.001295	0.000958	0.000729	0.003728	0.028239
8.000000	0.000795	0.000852	0.001123	0.000831	0.000634	0.003156	0.028405
9.000000	0.001028	0.001092	0.001426	0.001012	0.000754	0.004036	0.028185
10.000000	0.000914	0.000968	0.001267	0.000907	0.000670	0.003535	0.028284
11.000000	0.000790	0.000824	0.001106	0.000827	0.000667	0.003080	0.028426
12.000000	0.001053	0.001078	0.001413	0.001033	0.000746	0.004116	0.028151
13.000000	0.001076	0.001101	0.001414	0.001019	0.000727	0.004379	0.028090
14.000000	0.001028	0.001082	0.001421	0.001042	0.000763	0.004131	0.028160
15.000000	0.001183	0.001206	0.001552	0.001047	0.000782	0.004757	0.028001
16.000000	0.000920	0.001013	0.001341	0.001040	0.000786	0.003537	0.028265
17.000000	0.001220	0.001236	0.001583	0.001117	0.000794	0.004696	0.028011
18.000000	0.001121	0.001172	0.001525	0.001026	0.000754	0.004247	0.028089
19.000000	0.001113	0.001139	0.001455	0.001019	0.000717	0.004508	0.028064
20.000000	0.001161	0.001187	0.001546	0.001096	0.000787	0.004691	0.027999
21.000000	0.001054	0.001123	0.001456	0.001039	0.000789	0.004096	0.028119
22.000000	0.001179	0.001195	0.001532	0.001133	0.000821	0.004735	0.028008
23.000000	0.001013	0.001079	0.001439	0.001022	0.000745	0.003921	0.028200
24.000000	0.001053	0.001099	0.001445	0.001088	0.000833	0.004153	0.028146
25.000000	0.001264	0.001251	0.001628	0.001190	0.000846	0.004892	0.027953
26.000000	0.000861	0.000926	0.001240	0.000944	0.000729	0.003337	0.028319
27.000000	0.001019	0.001050	0.001380	0.001034	0.000733	0.003929	0.028169
28.000000	0.000866	0.000909	0.001195	0.000901	0.000664	0.003390	0.028345
29.000000	0.001161	0.001195	0.001530	0.001108	0.000809	0.004571	0.028013
30.000000	0.001215	0.001296	0.001688	0.001144	0.000814	0.004592	0.028000
31.000000	0.001285	0.001297	0.001675	0.001141	0.000822	0.005138	0.027875
32.000000	0.001212	0.001252	0.001652	0.001109	0.000820	0.004780	0.027971
33.000000	0.001048	0.001075	0.001397	0.001013	0.000755	0.004196	0.028136

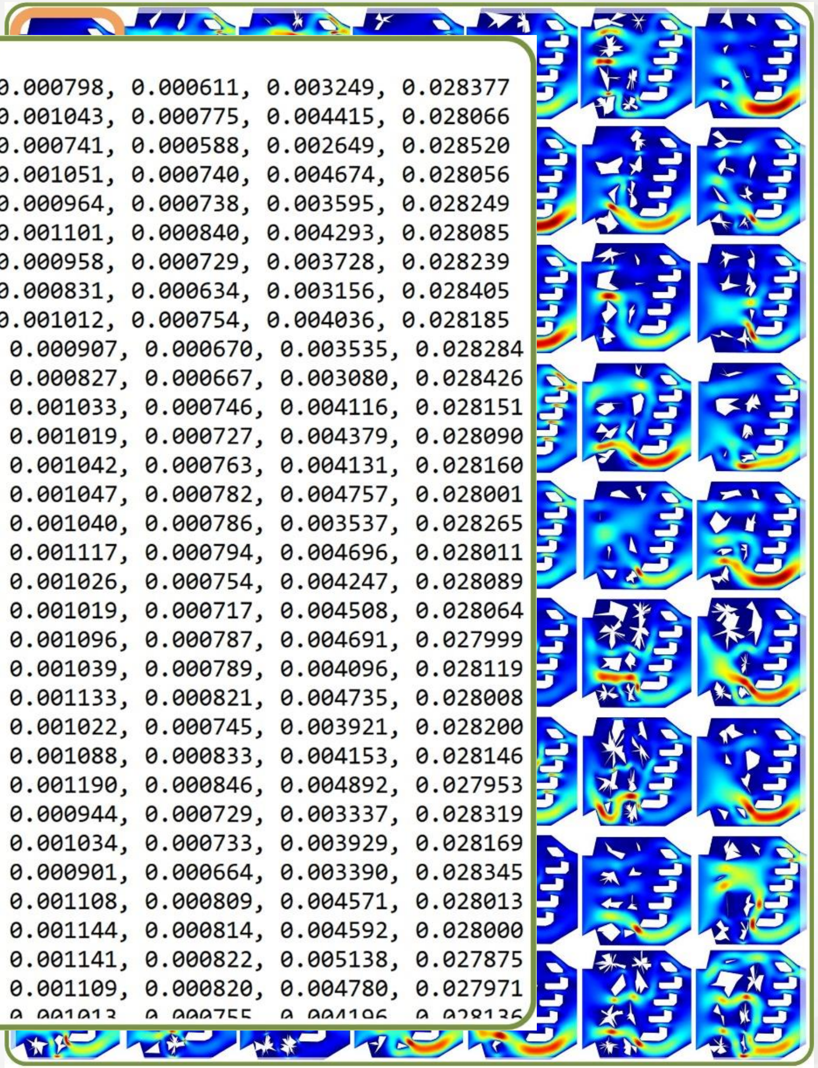

TOP. OPT. 3: EA, AUTO CREATION AND IMPROVEMENT OF 300 NEW GEOMETRIES

Generative design of microfluidic structures using evolutionary approach 1

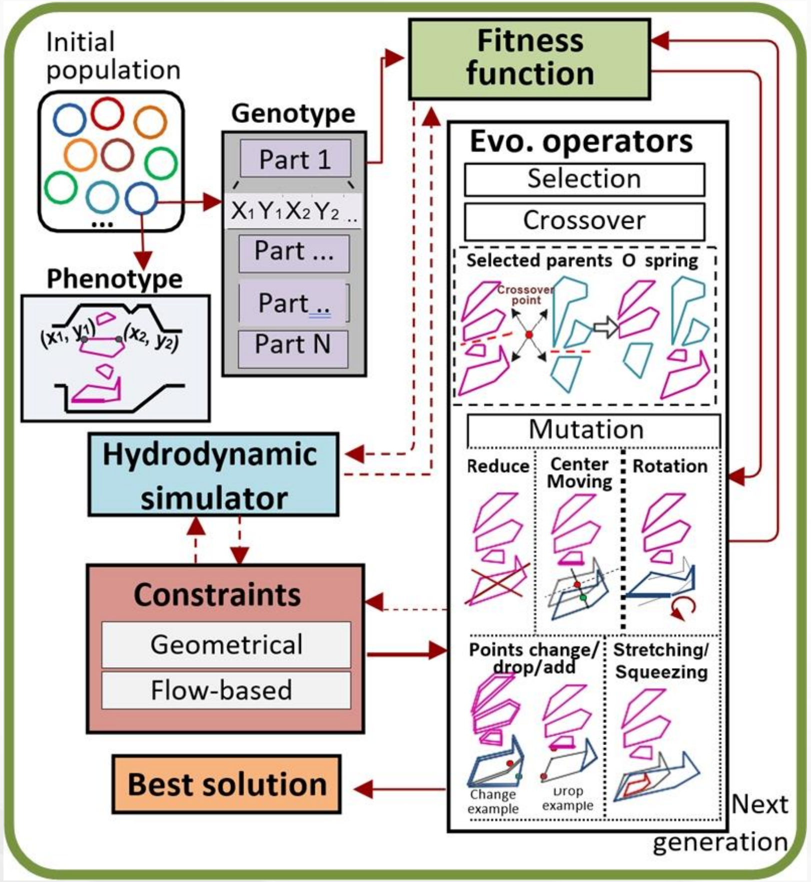

The scheme of evolutionary approach for the de- sign of microfluidic geometry and an example of problem- specific evolutionary operators.

$$X_{opt} = \arg\min_X F(X),$$
$$F(X) = G(F(Y(X))\,|\,G(X)),\ G(X) = (g_1(X), ..., g_M(X))$$
$$X = (P_1, P_2, ..., P_N),\ P = (Pt_1, Pt_2, ..., Pt_{k_i}),\ Pt_j = (x_j, y_j)$$

Nikitin,, .. **Grigorev** et al., GECCO 2021, Lille, France

Topology Optimization 3

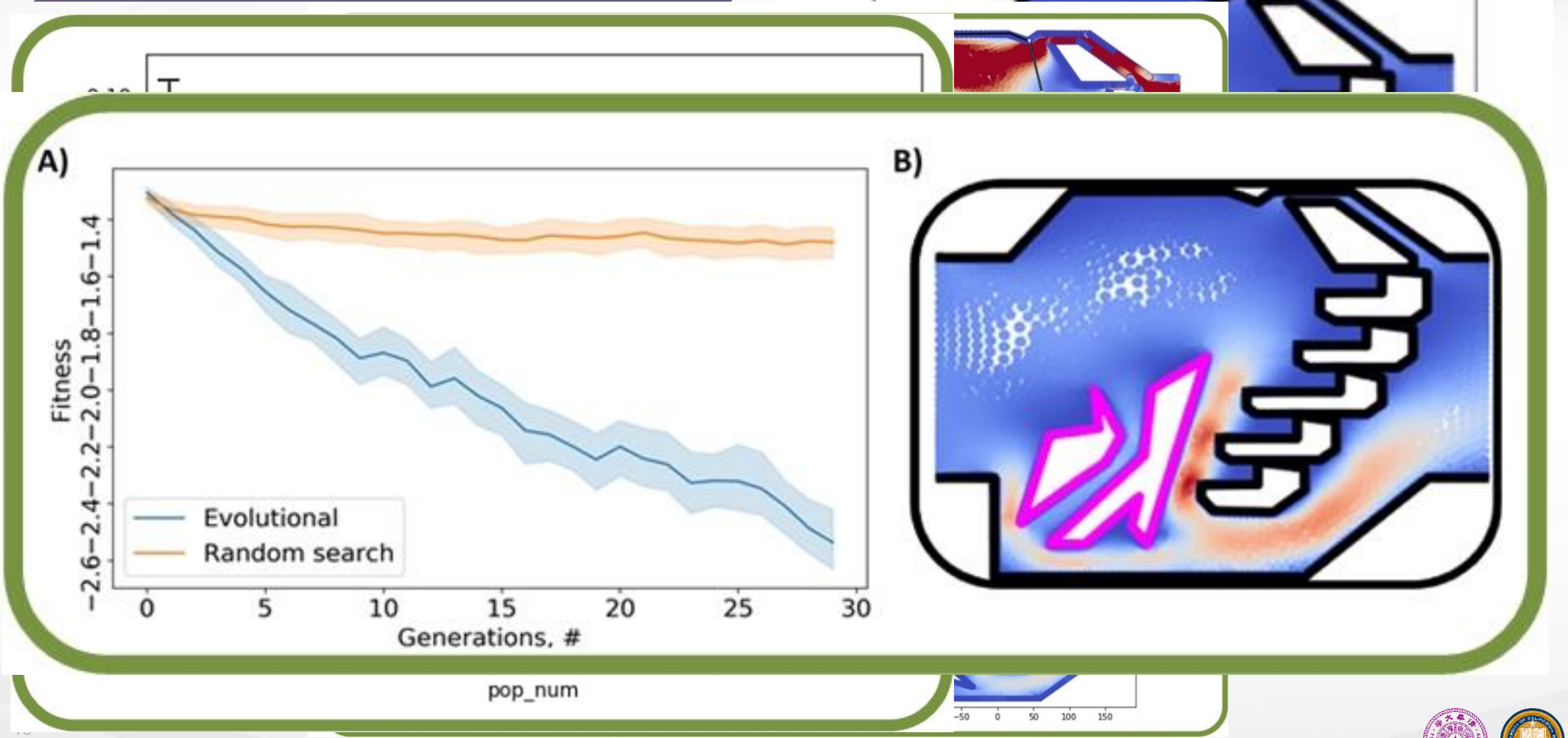

Nikitin,, .. **Grigorev** et al., GECCO 2021, Lille, France

TOP. OPT. 4: EA, AUTO CREATION SELF-IMPROVEMENT OF 30, 000 NEW GEOMETRIES

Design stages of cell traps and the architecture of the evolutionary algorithm

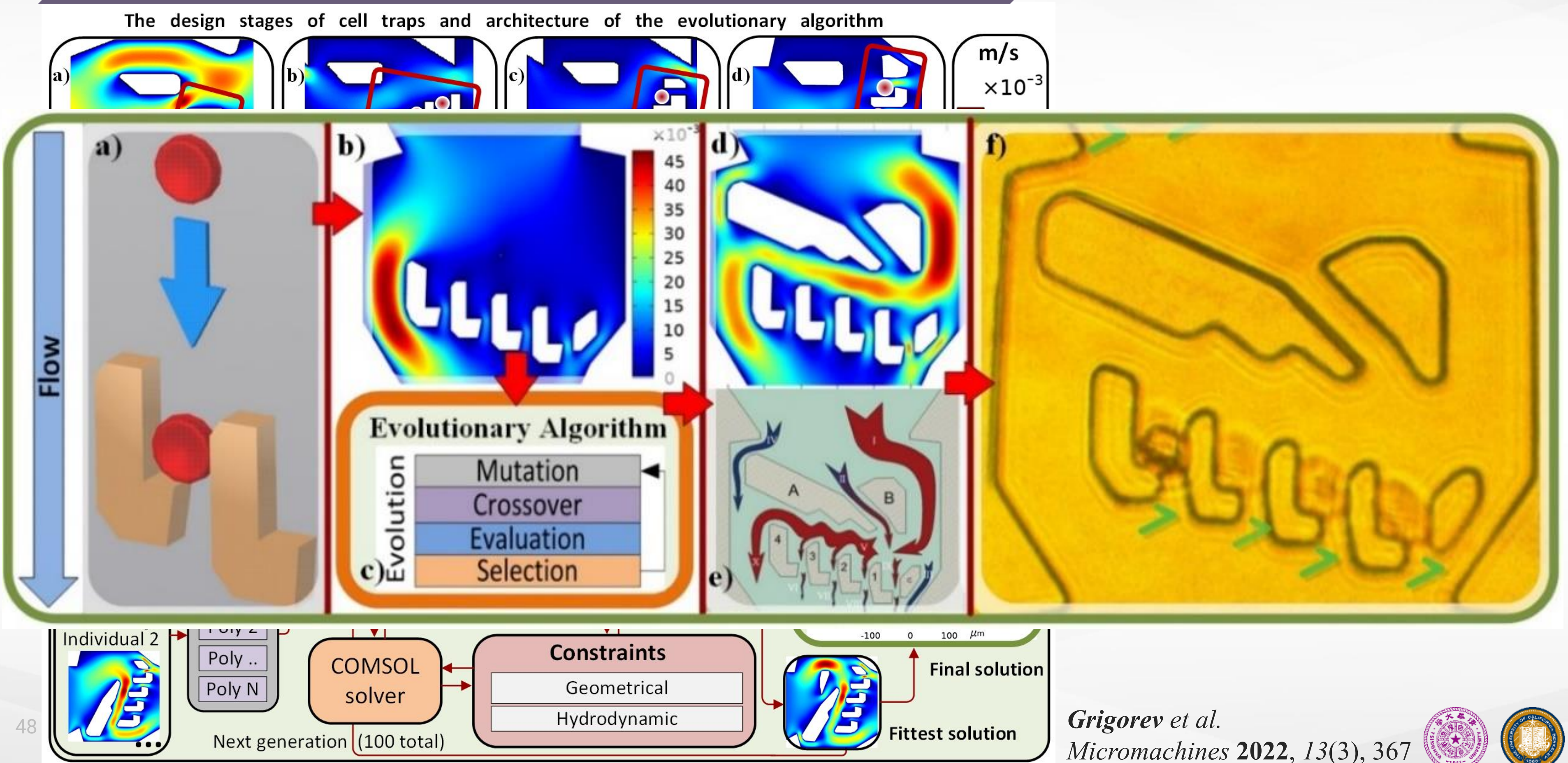

Grigorev et al.
Micromachines **2022**, *13*(3), 367

Constraints

CRL = maxop1(uy) + maxop1(vx)

$$\max_{\Omega}\left(\frac{\partial u}{\partial y}\right) + \max_{\Omega}\left(\frac{\partial v}{\partial x}\right)$$

CRV = intop1(abs(u^2 * vx - v^2 * uy + u*v*(vy - ux))/(u^2 + v^2)^1.5)

$$\iint_{\Omega} abs\left[\frac{u^2 * \frac{\partial v}{\partial x} - v^2\frac{\partial u}{\partial y} + uv * \left(\frac{\partial v}{\partial y} - \frac{\partial u}{\partial x}\right)}{(u^2 + v^2)^{3/2}}\right] dxdy$$

$$\boldsymbol{TVR} = \frac{\sum_{k=1}^{4} v_k}{v_{PD} + v_{main}}$$

Grigorev *et al.*
Micromachines **2022**, *13*(3), 367

Convergence graph

The convergence of the fitness function values (the function that is used to estimate how close a given design solution is to the specified aim) during the evolutionary optimization of cell traps for the 100 generations (iterations of evolution).

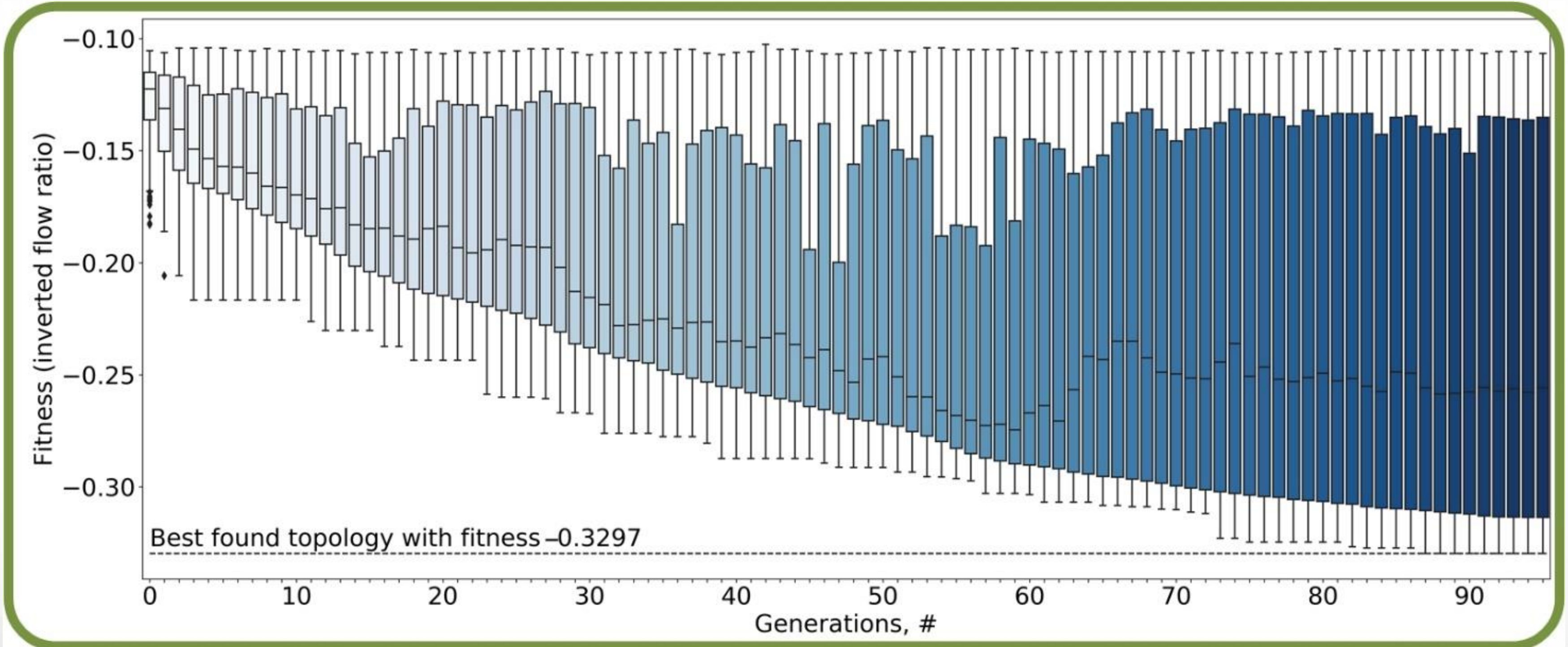

Grigorev *et al. Micromachines* **2022**, *13*(3), 367

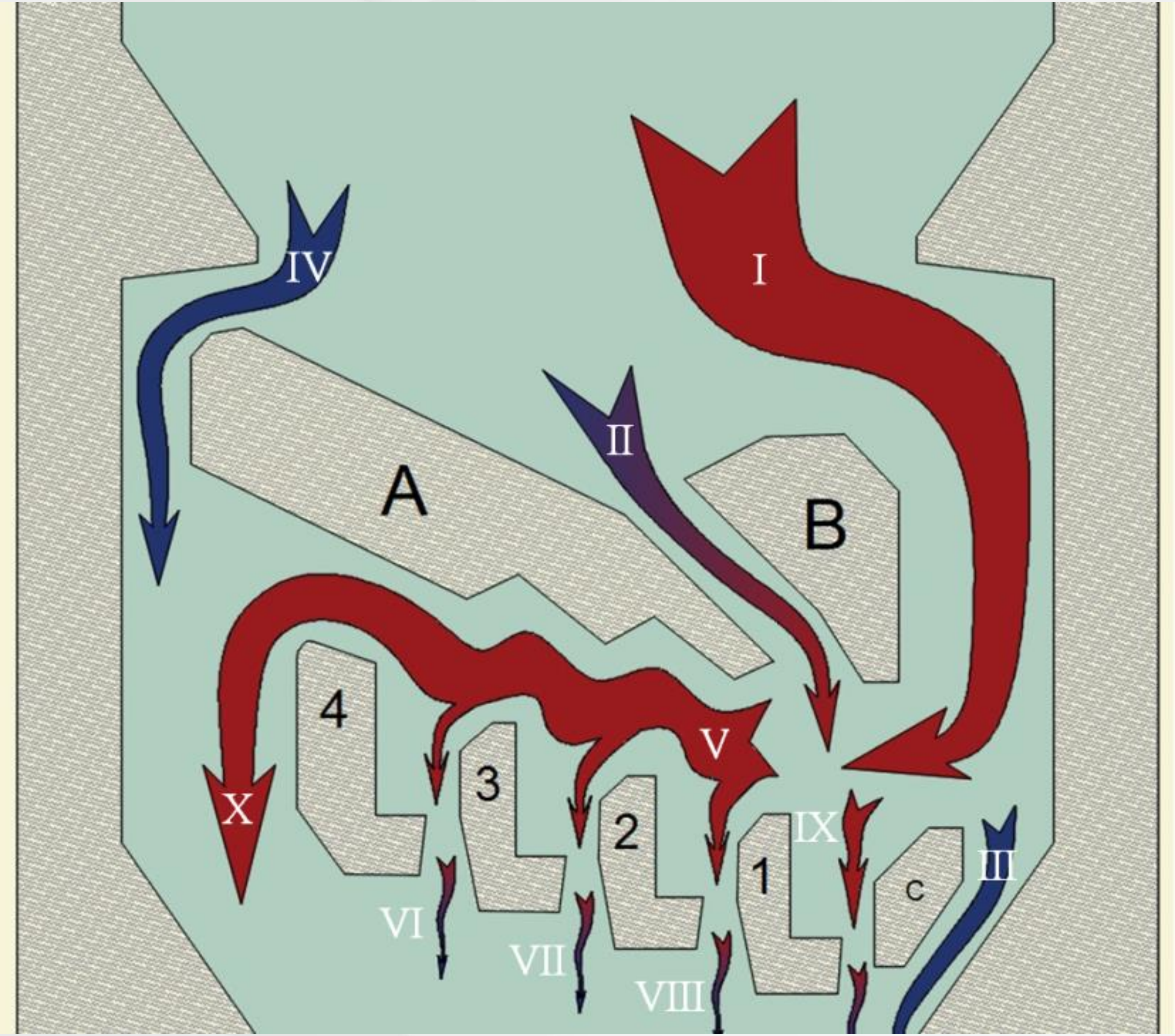

Final optimized geometry of the microfluidic trap for single cell

***Grigorev** et al.*
Micromachines **2022**, *13*(3), 367

Experimental results of the system following the evolutionary algorithm design to trap RBCs.

Parameter	Units	Initial	Target values	Optimized	Gain, %
vl_1	m/s	0.012038	determined	0.02308	**92**
vl_2	m/s	0.0094433		0.01579	**67**
vl_3	m/s	0.0094776	by	0.012701	**34**
vl_4	m/s	0.0095439		0.010092	**6**
vl_PD	m/s	0.0059983	TVR ratio	0.012438	**107**
vl_main	m/s	0.027247		0.019577	**−28**
CVR	1/m	70,769,000	< 7 × 10+07	17,113,000	**−76**
CRL	1/s	12717	< 30, 000	20615	**62**
TVR (target)	-	**1.22**	**1.22 < TVR < 2**	**1.93**	**58**

***Grigorev** et al. Micromachines* **2022**, *13*(3), 367

CONCLUSION AND CLOSING REMARKS

uFD design overview

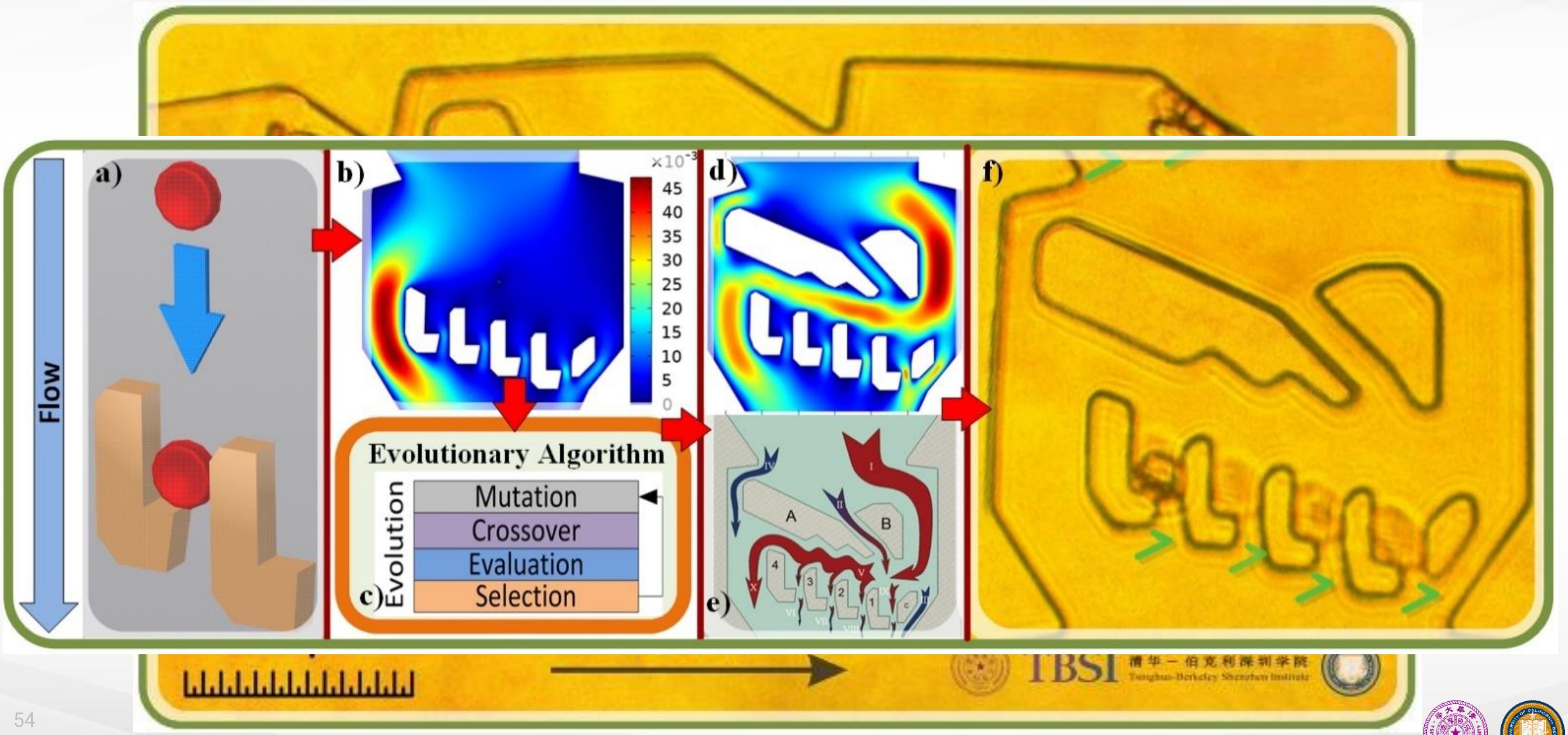

Grigorev et al. Micromachines **2022**, *13*(3), 367

Discussion

uFD successfully trapping cells

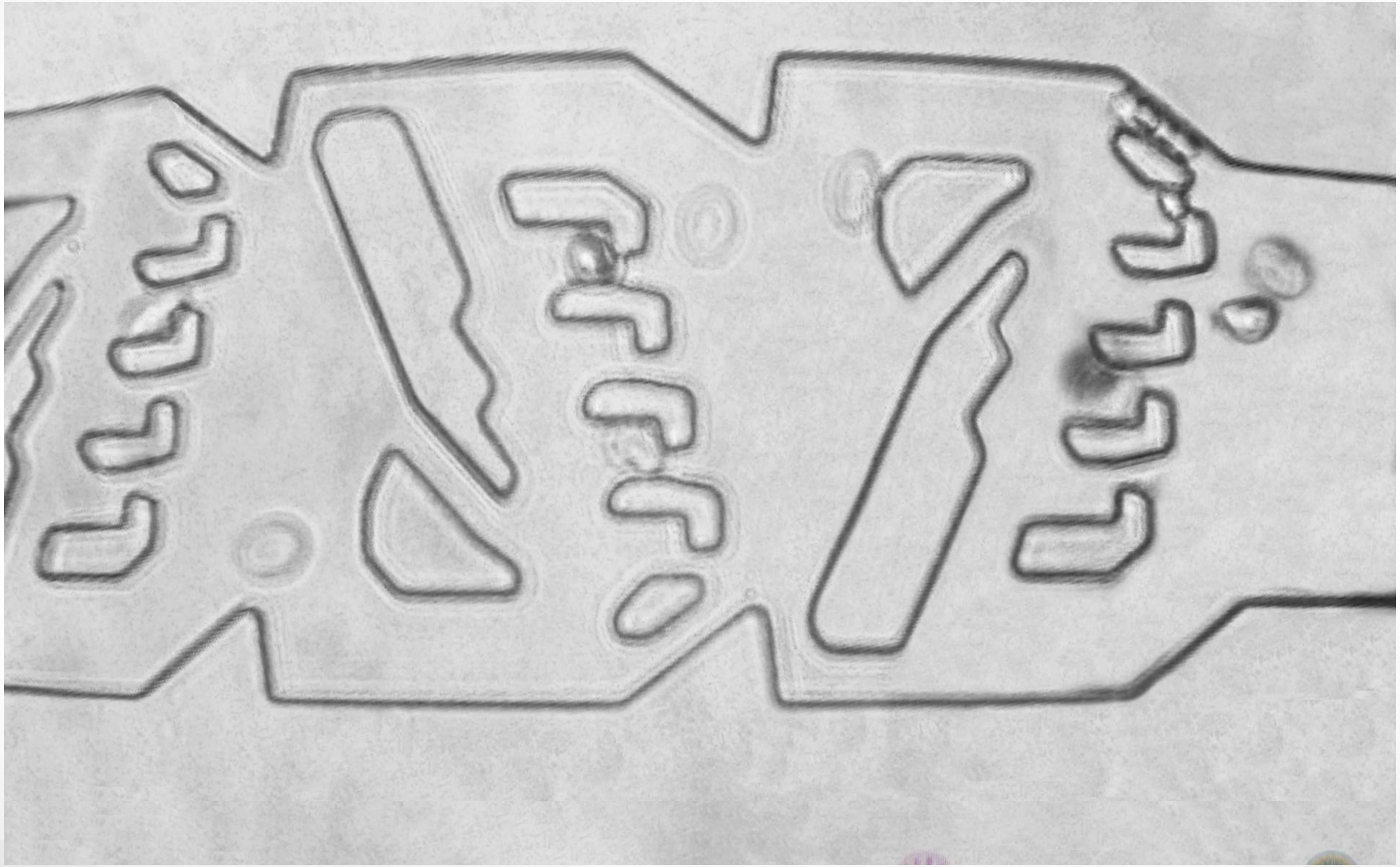

Grigorev et al. Micromachines **2022**, *13*(3), 367

References

References (498 refs)

1. G. Grigorev, W. Xiaohao and Q. Xiang, "Verification Of The Hypothesis Concerning The Optical / Rheological Properties Change Of A Clotting Native Blood Drop Correlated With The Erythrocytes Aging And Morphology Transformation Processes," *2019 IEEE International Conference on Real-time Computing and Robotics (RCAR)*, Irkutsk, Russia, 2019, pp. 531-536, doi: 10.1109/RCAR47638.2019.9043957.
2. Wood, Bayden & Caspers, Peter & Puppels, Gerwin & Pandiancherri, Shveta & McNaughton, Don. (2007). Resonance Raman spectroscopy of red blood cells using near infrared excitation. Analytical and bioanalytical chemistry. 387. 1691-703. 10.1007/s00216-006-0881-8.
3. Choi, S., T.G. Spiro, K.C. Langry, K.M. Smith, D.L. Budd, and G.N. La Mar. 1982. Structural correlations and vinyl influences in resonance Raman spectra of protoheme complexes and proteins. J. Amer. Chem. Soc. 104: 4345–4351.
4. Kitagawa, T., Y. Kyogoku, and T. Iizuka. 1976. Nature of the iron ligand bond in ferrous low spin hemoproteins studied by resonance Raman scattering. J. Amer. Chem. Soc. 98: 5169–5173.
5. Stein, P., I.M. Burke, and T.G. Spiro. 1975. Structural interpretation of heme protein resonance Raman frequencies. Preliminary normal coordinate analysis results. J. Amer. Chem. Soc. 97: 2304–2305.
6. G.N. Vishnyakov, G.G. Levin, V.L. Minaev, V.V.Pickalov, A.V. Likhachev, Microscopy and Analysis 18, 19 (2004).
7. *G.N. Vishnyakov, G.G. Levin, V.L. Minaev, M.M. Ermakov, 2018, published in Optika i Spektroskopiya, 2018, Vol. 125, No. 6, pp. 864–872.*
8. *Hou, X. (2017) Interplay between materials and microfluidics, Nat. Rev. Mater. doi:10.1038/natrevmats.2017.16*
9. *Nosrati, R. et al. (2017) Microfluidics for sperm analysis and selection, Nat. Rev. Urol. doi:10.1038/nrurol.2017.175*
10. Nawaz, A.A., Urbanska, M., Herbig, M. *et al.* Intelligent image-based deformation-assisted cell sorting with molecular specificity. *Nat Methods* (2020). https://doi.org/10.1038/s41592-020-0831-y
11. Alapan, Y., Little, J. & Gurkan, U. Heterogeneous Red Blood Cell Adhesion and Deformability in Sickle Cell Disease. *Sci Rep* 4, 7173 (2015). https://doi.org/10.1038/srep07173
12. Tao Luo, Jundi Hou, Shuxun Chen, Yu-Ting Chow, Ran Wang, Dongce Ma, Rong Zhu, and Dong Sun
13. Citation:, Microfluidic single-cell array platform enabling week-scale clonal expansion under chemical/electrical stimuli: Biomicrofluidics 11, 054103 (2017); doi: 10.1063/1.5000917
14. Thomas Borrvall∗;Joakim Petersson , Topology optimization of fluids in Stokes flow, International journal for numerical methods in fluids Int. J. Numer. Meth. Fluids 2003; 41:77–107 (DOI: 10.1002/?d.426)

Collaborations

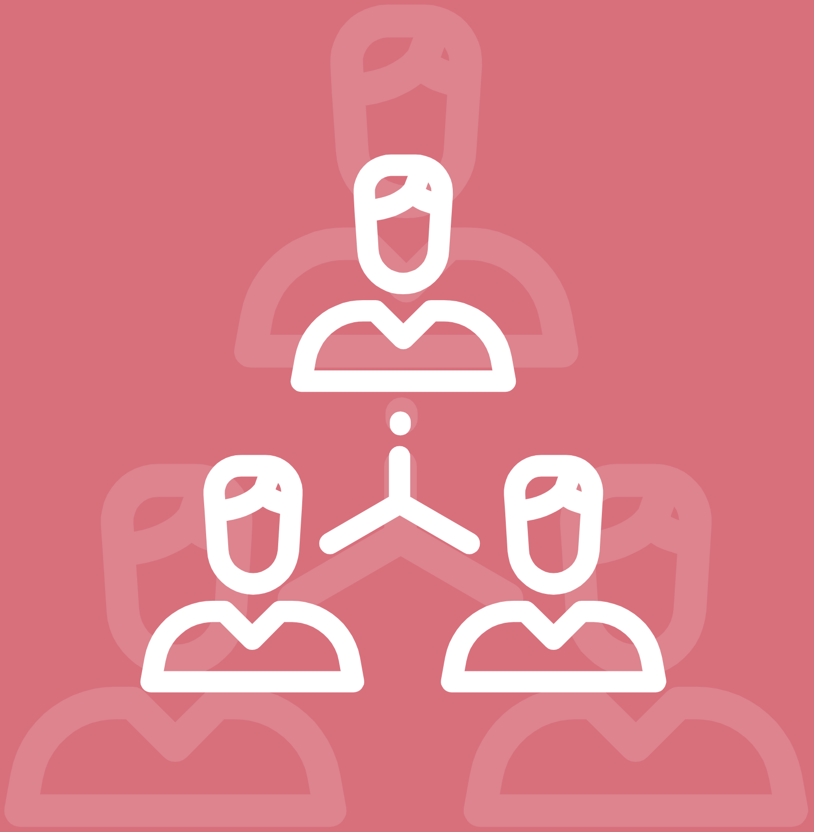

МГУ, M.V. Lomonosov's MSU, Biology School, Bio-physics department

- *Maksimov Georgii Vladimirovich*, professor, Core PI, department vice-director. Ph. D., Doctor of Biological Sciences;
- *Parshina Evgeniya Urievna*, senior PI, Ph.D.;
- Suchalko Oleg Ivanovich, Master student;

ВНИИОФИ,

- *Vis*
- *L* t;
- *E*

НИИО siology" of Russian **Academ**

- *M*
- *Ko*

ИТМО

- *Ka*
- *Ni*
- *Hv*

中国科

- *Sh*
- *Fe*

深圳

- *M* ogical Sciences;
- *T*

Stanfor

- *Sayk*
- *Kapitu*

深圳北理莫斯科大学, **Biophysics dep**

- *Maksimov Georgii Vladimirovich*, professor, Core PI, department vice-director. Ph. D., Doctor of Biological Sciences;
- *Tarasov Alexei Borisovich*, professor, Core PI, Dean. Ph. D.

清华大学，Tsinghua University, MEMS Lab

- *王晓浩*, professor, Core PI, department vice-director. Ph. D., Doctor of Biological Sciences;
- *钱翔*, senior PI, Ph.D.;
- Labmates, students, postdocs, research fellows.

University of California in Berkeley, Lin's Lab

- *Lin Liwei*, Core PI, Ph. D. TBSI vice-president, Lab Head;
- Labmates, students, postdocs, research fellows.

Future work

Future development of EA based on Generative Adversarial Networks

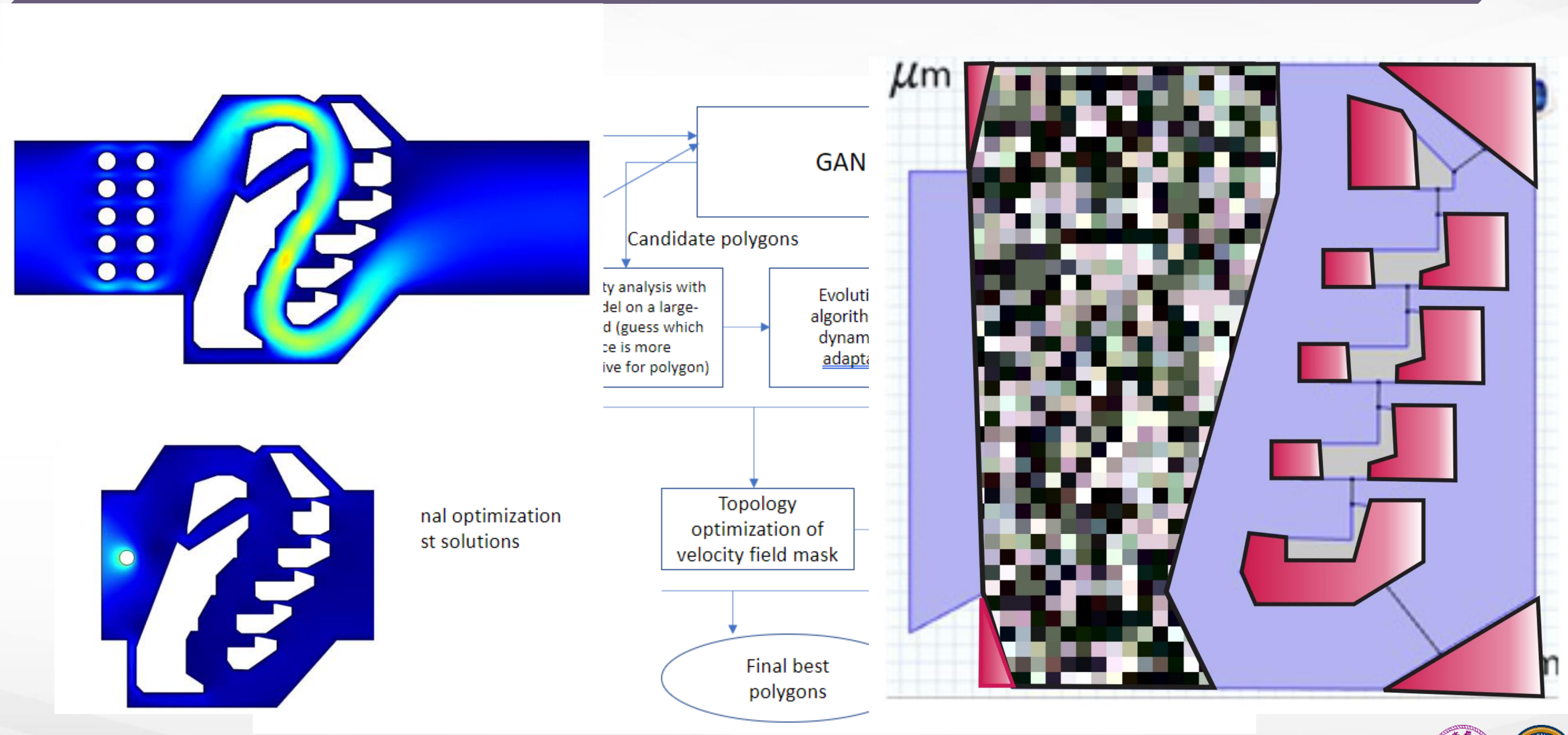

Благодарю за внимание!

懇請各位老師批評指正